Spatio-temporal modelling of human-caused fire in the Mount Kenya region

Master thesis
of
Gergo Dioszegi, BSc

for obtaining the academic degree of Master of Science (MSc)

Supervisor
Harald Vacik, Ao. Univ. Prof. Dipl.-Ing. Dr. MAS

Submitted in March 2018 to the
Institute of Silviculture
Department of Forest- and Soil Sciences
BOKU - University of Natural Resources and Life Sciences

Index

...hic et nunc, because

fire never sleeps...

for my Mother

List of abbreviations

AF1 -   After Fire 1 (IC)

AF2 -   After Fire 2 (IC)

ASF -   Alaska Satellite Facility

CSR -   Complete Spatial Randomness

ETM+ -   Enhanced Thematic Mapper Plus

FFS -   Future Forest Stations

FO -   Fire Occurrence, Fire Occurrences

IC -   Ignition Classes

IP -   Ignition Point, Ignition Points (IC)

IS -   Ignition Source, Ignition Sources

ITCZ -   Intertropical Convergence Zone

KDE -   Kernel Density Estimation

KEFRI -   Kenya Forestry Research Institute

K-S test -   Kolmogorov-Smirnov test

KFS -   Kenya Forest Service

MODIS -   Moderate-resolution Imaging Spectroradiometer

MMD -   Minimum Mean Distance

MKFR -   Mount Kenya Forest Reserve

MKNP -   Mount Kenya National Park

NBR -   Normalized Burn Ratio

NDVI -   Normalized Difference Vegetation Index

NTH -   Nearest Neighbour

PID -   Pixel Ident Distribution

PPMCC -   Pearson's Product Moment Correlation Coefficient

RS -   Remote Sensing

SAC -   Moran's I Spatial Autocorrelation

SPPA -   Spatial Point Pattern Analysis

U -   Unclear (IC)

USGS -   US Geological Survey

VegReg -   Vegetation Regeneration

VMR -   Variance to Mean Ratio

List of figures and tables

Abstract

Wildfires are major threats to Mt. Kenya forests and its unique afro-alpine ecosystem. The main ecosystem service, securing the steady supply of enough fresh drinking water with sufficient quality is at risk. For assuring the sustainable provision of this forest function several scientific studies with different scope have been implemented to understand the fire regime in the area.

The present thesis quantified the spatial characteristics of fire events for the period of 2000-2015, to reveal the underlying patterns of its fire regime. Human activities relating to spatial patterns of fire were identified, and the effects of these patterns on the fire regime were assessed. Analyses were performed using diverse remote sensing and GIS data. The quality and quantity of these data providing information about the fire regime allowed assessing the applicability of remote sensing data and spatial analysis techniques for supporting an integral fire management.

Clustering pattern at very short and short distances, bimodal seasonality, and fire ignition point dependency on road and trail density are the main characteristics of the Mount Kenya fire regime. Frequent small fires burn in the forest, while less frequent larger fires dominate the high altitudinal moorland. The vegetation around Mount Kenya is adapted to fires and is actively regenerating in the landscape.

The available remote sensing data could be used along with the improved GIS data for more specific studies, giving recommendations for adapting forest management, and developing fire danger maps.

Abstract (~deutsch~)

Waldbrände sind eine große Bedrohung für den Schutz der Wälder Mt. Kenyas und ihres einzigartigen Ökosystems. Die wichtigste Ökosystem-Dienstleistung, die regionale Sicherung einer ausreichenden Trinkwasserversorgung mit bester Qualität ist gefährdet. Um diese wesentliche Waldfunktion zu erhalten, sind zahlreiche wissenschaftliche Studien mit unterschiedlichem Kontext durchgeführt worden, um die Bedeutung von Waldbränden die zu untersuchen.

Die vorliegende Arbeit quantifiziert die räumlichen Charakteristika der Brandereignisse für den Zeitraum 2000-2015, und untersucht die zugrunde liegenden Muster des Feuerregimes. Menschliche Aktivitäten in Bezug auf die identifizierten räumlichen Muster der aufgetretenen Brände wurden identifiziert, und deren Bedeutung für das Feuerregime wurden bewertet. Analysen wurden mit diversen Fernerkundungs- und GIS-Daten durchgeführt. Die Beurteilung der Qualität und Quantität erlaubte eine Einschätzung über die Anwendbarkeit von Fernerkundungsdaten und räumlichen Analysemethoden zur Unterstützung einer integralen Bewirtschaftung von Waldbränden.

Es wurden räumliche Cluster auf sehr kurzen und kurzen Entfernungen, eine bimodale Saisonalität und eine Abhängigkeit der Brandherde von Straßen- und Wege-Dichte als wesentliche Merkmale des Feuerregimes am Mt. Kenya festgestellt. Oft vorkommende kleinere Brände treten häufiger im Wald auf, während selten auftretende größere Brände häufiger das Hochmoor dominieren. Die Vegetation am Mount Kenya ist angepasst an die auftretenden Brände und regeneriert sich ständig.

Die verfügbaren Fernerkundungsdaten könnten gemeinsam mit den verbesserten GIS-Daten für weiterführende Studien verwendet werden, um Empfehlungen für eine angepasste Waldbewirtschaftung zugeben und entsprechende Gefährdungskarten zu erstellen.

1. Introduction

Fire and different fire systems have been playing an important role of environmental changes for billions of years [1]. The last 60000 years have witnessed a rapid growth and differentiation of human land use activities in which human caused fire became a more and more significant factor [2]. In one of the oldest historically known religion, Zoroastrianism, fire (azar) is considered to be an ethereal medium through which pure wisdom and spiritual insight can be obtained. Humans have a rather two-dimensional relationship with fire: it could be either beneficial or destructive, or both at the same time. Fire itself, however, shows a multi-dimensional character strongly dependent on environmental variables, such as temperature, precipitation, wind or air humidity, which suggests that fire ignition can be predicted along well assessed environmental gradients. Fire regime determined by different combinations of fire characteristics -intensity, frequency, seasonality, extent, size- can be used for spatial fire pattern analysis to see if there is any repeating pattern at a given location in space. One of the most researched topic of fire ecologists is the history, change and prediction of local and global human induced fire events. In our modern time, remote sensing (RS) and GIS became indispensable for any fire-landscape relation (spatial) analysing project [3]. When in the early 90's the availability of satellite data "extended" research capabilities, the large number of African fire occurrences surprised the scientific world [4].

The present study focusses on a specific ecosystem: the Mount Kenya region. This tropical alpine area with its vegetation plays a life sustaining role in fresh water supply for its wide surroundings [5, 6, 7]. The intact keeping of fresh water production is crucial for humans and animals alike. Besides its hydrological function, this "water tower" maintains a unique composition of biodiversity found only on the African continent. In search of potential drivers of climate change, the tree line change was analysed in tropical African highlands [8]. In case of Mount Kenya the tree line (~3400 m) tends to move downward and it is regulated by anthropogenic caused fires [8, 9, 10]. Indeed, according to a recent study the last 16 years have witnessed fires with a shifting fire regime on the moorland, above the tree line, hindering the trees from an uphill succession [11]. The human impact on fire ignition is a global phenomenon that alters the spatial extent of wildfire in all biomes of the Earth system [12, 13]. The dimensions of altering depend not only on human activities but on environmental variables such as regional climate, vegetation association, on physical environments and the scale of space and time of assessment. Within the East-African alpine zone Mount Kenya and its ecosystem, due to adjacent densely populated areas and human land use activities, is very vulnerable to fires. It has to be noted that fire can also be constructive in terms of being "responsible for maintaining the health and perpetuity of certain fire-dependent ecosystems" [4]. To my knowledge has fire dependency of this afro-alpine system never been studied so far.

Fire ignition sources are manifold, Nyongesa [7] and Ngugi (written comment) agree on the following major causes of wildfire: human activities during farmland preparation within some forest stations, practicing illegal charcoal burning (Nyongesa, written comment), arson, poaching and honey harvesting. Livestock grazing counts also as one of major sources of ignition, because it is allowed in plantations (within forest stations) all around the year [14].

According to Ngugi (written comment) grazing is more intensive during the dry period of the year, from January to March respectively.

Natural forest cover (2 % of the whole country) remaining in Kenya is under regulation of governmental institutions [15]. With fire becoming an integral component in Mount Kenya ecosystem [7, 11, 16], a cooperative platform between Mount Kenya National Park (MKNP) and the Kenya Forest Service (KFS) can be the framework for implementing a fire management plan. It is vital in securing a sustainable preservation of this ecosystem and to ensure that there will be fresh water available in quantity and in good quality for future generations.

Fire ignition cause is estimated to be mainly human [7, 11, 16]. However, the relation between fire and the human footprint has never been mapped in the Mount Kenya ecosystem before. Therefore, this study is trying to unlock the spatial secrets of the regional fire regime and its direct human relation in a 15-year time scale. Indirect anthropogenic impact is assessed through burnt area, combined vegetation regeneration-burn severity and Normalized Difference Vegetation Index (NDVI) analysis. The dual-season hypothesis of Poletti [16], who examined the period between 1980-2015, has recently been challenged by Downing et al. (study period: 2000-2015) stating that the bimodal fire season profile changed to a single fire season around 2004. It is important to note that the former study concentrated on fire prone forest area, while the latter one has the "high"-moorland in focus. So, this thesis tries to reveal the characteristics of fire regime and its underlying processes, assuming dual-seasonality (based on the works of above mentioned authors) and using available RS data for the (by the extent of fire occurrences defined area) Mount Kenya region.

The general objective of the thesis at hand is to clarify by analysing diverse RS and socio-economic data set the relationship between fire regime and human activities in order to help setting the fundaments of fire management for KFS and MKNP. Therefore, the following questions are to clarify:

(I) What are the spatial characteristics of the Mount Kenya fire regime and how can they be quantified?

(II) Which spatial patterns can be identified in relation to human activities (direct-ignition source and indirect-burnt area, fire severity, vegetation regeneration and NDVI) and how fire regime (I) is effected by them?

(III) How is the quality and quantity of available remote sensing (RS) data to provide necessary information relating questions (I) and (II) above?

2. Materials and methods

2.1. Study area

The geographical boundary of this study is the forested area (the green belt between 1400-2000 m and ~3400 m) of Mount Kenya within the forest stations and its marginal fire-ecologically inseperable area: the moorland above ~3400 m, belonging to Mount Kenya Reserve (MKR). The total area of the Mount Kenya Reserve is 263200 hectares (=2632 km^2).

Mount Kenya's equatorial mountain climate is strongly influenced by precipitation. The Intertropical Convergence Zone (ITCZ, the low-pressure belt along the Equator) is marked with heavy rainfalls. The long-lasting rain period (from the middle of March to the beginning of June) and the short-lasting rain periods (from the middle of October to December) define the dry-wet changing seasonality of Mount Kenya [17]. The amount of rainfall is distributed differently in the region, from an average precipitation of 900 mm/year in the North to 2300 mm/year in the South-Eastern regions.

With its 5200m high soaring peak, is Mount Kenya the second highest mountain on the African continent. Its east-central, equatorial location in the middle of Kenya, is home to about 200.000 hectares of unique afro-alpine forest cover [18]. The main vegetation communities are moorland, forest belt, wooded grassland, and cropland. The moorland lies between 3000 m and 3500 m, it is referred to as Ericaceous belt [19] and is mainly covered with giant heath, the African sage (Artemisia afra) and several Gentians (Swertia spp.). Indigenous forest starts at 2400 m down to 2000 m and dominated by Podocarpus latifolia. At lower altitudes (down to the lower boundary of the forest belt ~ 1400m) the species change depending on aspect. Wooded grassland concerns both plantations (in the vicinity to the lower boundary of the forest) and the vegetation between the moorland and the forest, the so called inner areas. Plantations are "cultivated" according to shamba system with little trees mixed with cropland. The main cultivated species on the cropland are vegetables such as potatoes, maize, tomatoes. Tea is also cultivated on the lower southern slopes of the mountain, but these cultivations lie outside of the Forest Reserve territory [19].

The Mount Kenya massive emerged from diverging activities of the Great Rift Valley and is part of the volcano chain, forming the highest peaks of the continent. The upper part of the extinct volcano is under administration of Mount Kenya National Park (MKNP) and the lower (up to ~3400 m) forest belt, divided into forest stations (Fig. 1), falls to jurisdiction of Mount Kenya Forest Reserve (MKFR), operated by the Kenya Forest Service (KFS). As mentioned above, both areas belong to the MKR. The institutions responsible for forest management are the KFS station administrations.
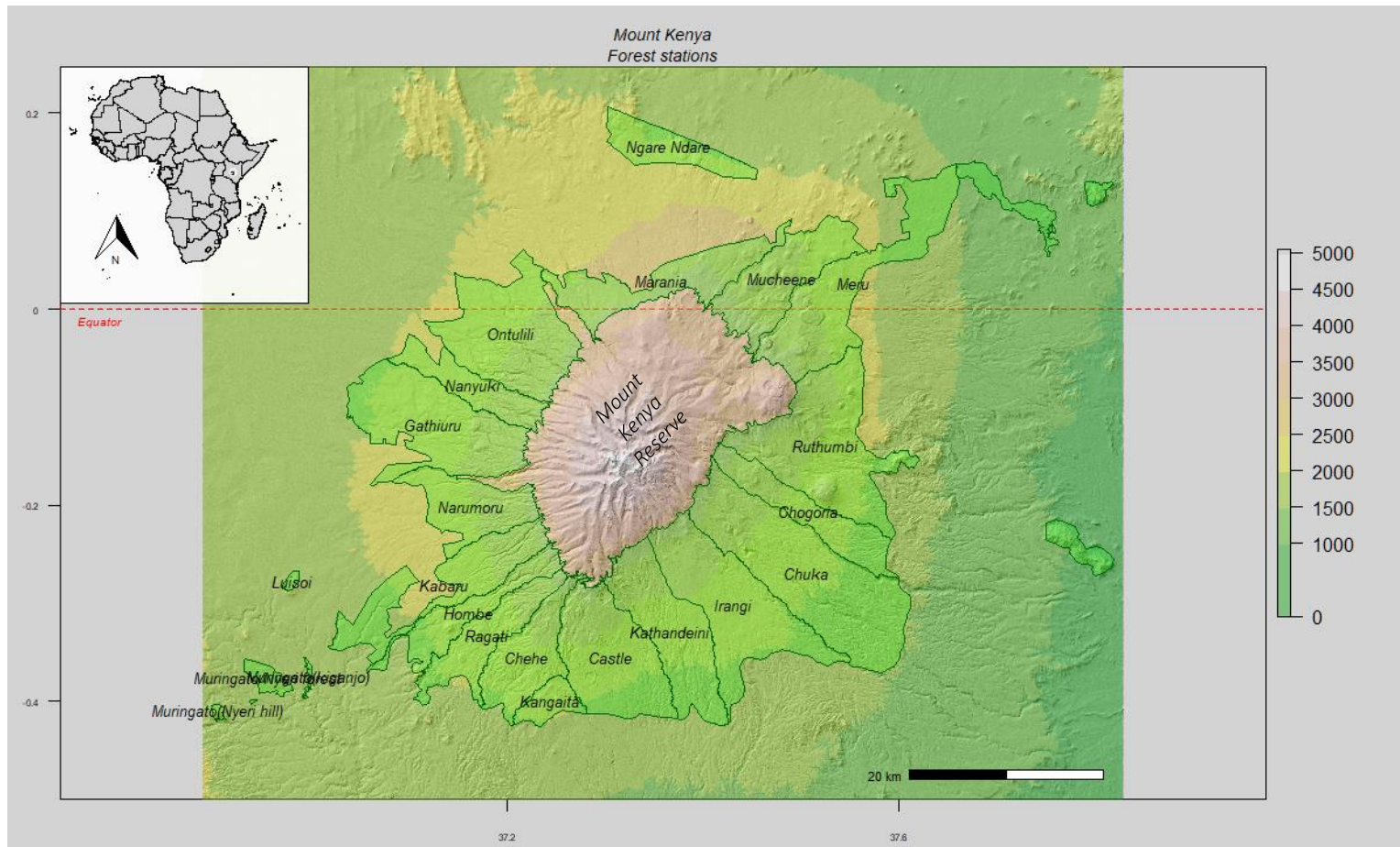
Fig. 1. Mount Kenya region and the Mount Kenya Reserve including the upper moorland and the forest station administrations.

2.2. Data set

2.2.1. Firemaps

Wide range of data was prepared and given by the Mount Kenya Team (group of researchers) who worked within the framework of FIREMAPS project in cooperation with the Kenya Forest Service and the Kenyan Forestry Research Institute (KEFRI). The FIREMAPS folder provided, contains various climate data such as temperature, precipitation, relative air humidity and wind speed. All data measured in five meteorologic stations located on the North/North-west side of the studied area, adjacent to but far outside of the forest stations. GIS applicable data included (more details in the following chapter) a core zone shapefile encompassing municipality land around the lower boundaries of the forest stations and the higher elevated moorland, was supposed to serve as the original borderline of interest area. This buffer zone gives the extent to road density and sub-district (municipality land) files. A Boolean vegetation map (Fig. 2.) with 30 m spatial resolution was also included. Furthermore, collected socio-economic data such as sub-district based population density, district based literacy and land use indicating data are also part of the data set.
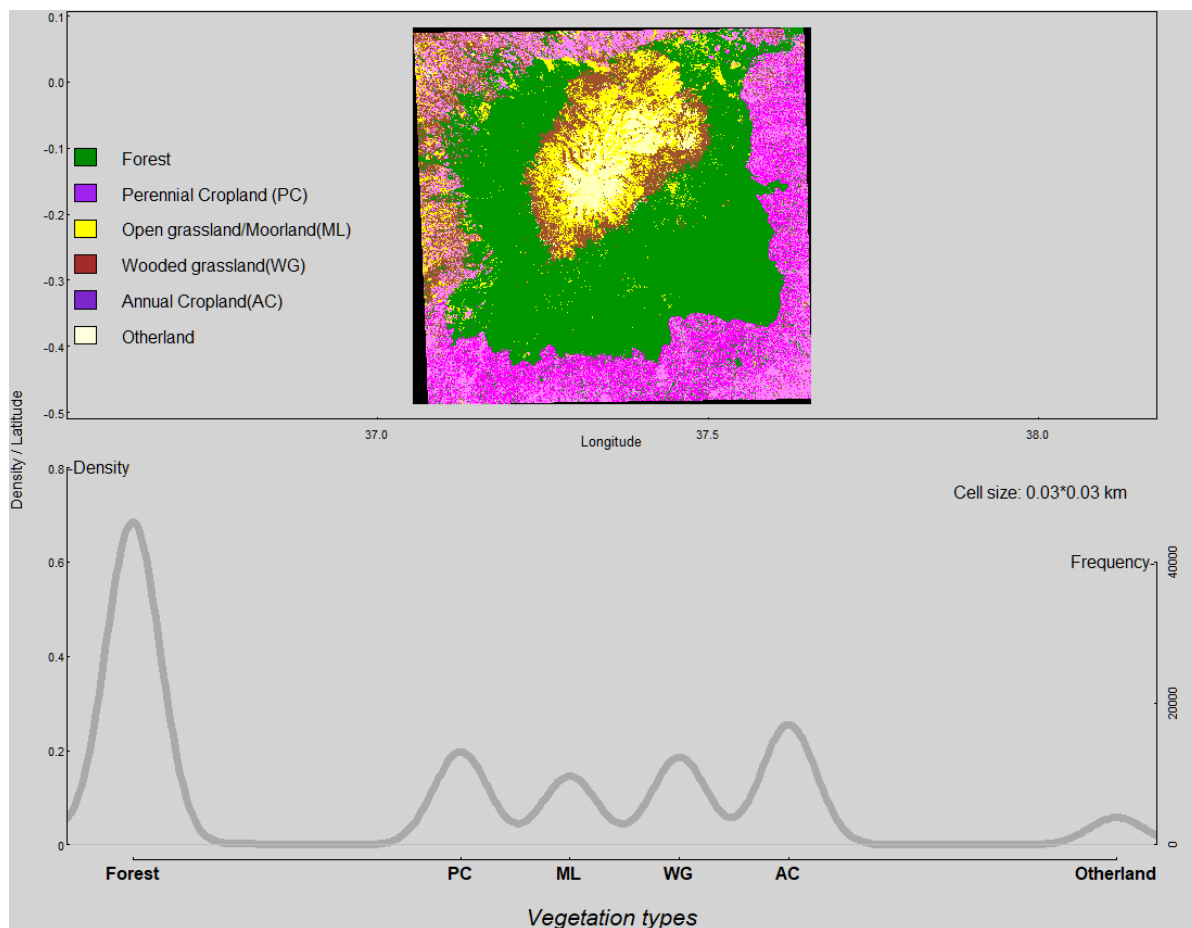
Fig. 2. Vegetation classes and their density distribution in the Mount Kenya region (Source: Kenyan Forestry Research Institute).

2.2.2. RS and GIS

Mapping fire occurrences and constructing fire regime in a combined spatial and timely context, requires good quality RS data.

The overall fire detection performance of Collection 5 Terra MODIS is on global scale acceptably accurate [20, 21, 22, 23]. For fire regime reconstruction MODIS MCD14DL - Collection 5 data is widely used. With a very low false alarm rate (under 1 %) in Central-Africa it promised to be very accurate, however, the satellite can miss smaller fires under cloud or fraction tree cover [24]. MODIS 5 data set was prepared and given by KEFRI in GIS applicable shapefile (shp) format.

Accuracy of Collection 6 MCD64A1 500-m Burned Area Product was promising [25]. However, as shown by a case study [26], Collection 5 MCD54A1 Burned Area Product is a better performer in detecting small fires that occur frequently in a steep mountainous area. Accordingly, the latter product was selected for the burnt area assessment.

Both data set are available from 2000 and can freely be downloaded from the MODIS website. For estimating and mapping burn severity, NDVI and vegetation regeneration 30 m spatial resolution Landsat 7 ETM + and 8 images were used, provided by the US Geological Survey (USGS). Satellite images based burn severity analysis have recently gained more ground in research due to their application for reproducing fairly accurate above ground biomass

5

changes [27]. Ancillary data, 12,5 m spatial resolution digital elevation model images were downloaded from the Alaska Satellite Facility (ASF) website. As far as Lidar point cloud data concerned, all efforts of obtaining them bore no fruits, partly because there is not many in the whole country, partly because of the existing ones of Aberdare Range (located occidental to Mount Kenya) are not directly relevant to the studied area.

Source	Spatial resolution (m)	Period/Date	Content
MODIS https://earthdata.nasa.gov/c5-mcd14dl	-	2001-2015	MODIS 5 fire occurrence (shp)
MODIS ftp://ba1.geog.umd.edu/	-	2001-2015	MODIS 5 Burnt area product (shp)
USGS https://earthexplorer.usgs.gov/	30	21.02.2000	Landsat 7 ETM+ satellite image
USGS	30	28.03.2016	Landsat 8 satellite image
ASF https://vertex.daac.asf.alaska.edu/	12.5	-	Digital elevation model (DEM) images

Table 1. RS data used in this study. - indicates irrelevance.

2.3. Methodology

2.3.1. On mapping fire

First of all, various spatial analyses were applied using ArcGIS to assess the relationship between fire occurrences (FO) and several socio-economic variables such as population density, animal grazing, honey collecting, illiteracy and education level. The seasonality of FO and their spatial and temporal dispersal was also mapped to get the first insight in FO behaviour. Some basic maps were created in order to utilize them in organized workshops where different stake-holders discussed planning options of a fire preventive adopting management in the study area.

After the first steps, the author decided to change for R software environment due to spatial statistical power of the *spatstat* package. FO were divided in frequency classes to address fire regime's monthly temporal distribution. To evaluate spatial relationship/connectivity of FO various analyses of an advanced Spatial Point Pattern Analysis (SPPA) were executed. The results of SPPA were mapped accordingly. Moreover, the maps of burnt area, Normalized Difference Vegetation Index (NDVI), the combined vegetation regeneration and burn severity analysis were also realized in a similar way. All maps (except the last one in the recommendation chapter) were finalized using diverse combinations of RS, GIS related and other packages (*adehabitatMA, rgdal, raster, rasterVis, maptools, sp, prettymapr, spdep, rgeos, GIStools, devtools, RStoolbox, colorspace, RColorBrewer, lattice, satellite, rLandsat8* and *landsat*) in R computational environment. It has to be noted that

ArcGIS remained in application for preparatory purposes and for calculating burnt area.

All analyses, mapping as well as modelling of the present thesis are considering the non-boundary behaviour of fire and are conducted with focussing on the spatial dispersal of FO.

2.3.2. On spatial analyses

In the framework of **Spatial Point Pattern Analysis (SPPA)** Variance to Mean Ratio analysis, G- and K-function methods plus Kernel Density Estimation were carried out so as to quantify and qualify density, spatial and temporal distribution of FO assuming double seasonality.

(1) Fire density combined with dispersion index, the ***Variance to Mean Ratio*** (VMR): by analysing the distribution of defined (5 km^2), superimposed quadrats, the point pattern arrangement can be verified. In quadrats, the variance index, called VMR standardizes the degree of variability of cell frequencies in relation to mean cell frequency [28]. The calculation is based on

$$VMR = \frac{\text{VAR}}{\text{MEAN}}$$

where variance is concepted by the formula

$$VAR = \frac{\sum f_i * x_i^2 - [\frac{(\sum x_i * f_i)^2}{m}]}{m-1}$$

and the mean as

$$MEAN = \frac{n}{m}$$

n = number of points

m = number of quadrats

f_i = frequency of quadrats

x_1 = number of points per quadrat.

(2) A more objective method (no self-defined superimposed quadrat), the ***G-function*** was conducted to get more insight into spatial characteristic of FO. It is an exploratory analysis, one of the distance methods, estimating the nearest neighbour distance distribution function. It is a statistic summarising approach aiming at spatial regularity / clustering of points. The estimate of G is compared to its 'original' true value for complete spatial randomness (CSR), expressed as a *homogenous Poisson point process*, which is

$$G(r) = 1 - \exp(-\lambda * \pi * r^2)$$

where λ signifies the expected number of points per unit area and *r* is the distance (the mean minimum distance of all points to their nearest ones) at which *G(r)* is computed [29, 30].

(3) *Ripley's K-function*: a statistic approach of analysing aspects of inter-point dependence or non-dependence, spatial point regularity or irregularity, respectively [31, 32]. The estimate of K is compared to its 'original' true value for complete spatial randomness (CSR), a *stationary Poisson point process*, which is

$$K(r) = \pi * r^2$$

The estimate of K(r) is calculated with the form

$$K(r) = (a/(n * (n\text{-}1))) * \sum[i,j] \ I(d[i,j] <= r) \ e[i,j])$$

where

a = area of the window

n = number of points

d[i,j] = distance between two points

I(d[i,j] <= r) = 1 if the distance is $\leq r$.

e[i,j] = edge correction weight (only in case of large point pattern > 1000 points).

(4) *Kernel Density Estimation* (KDE): a non-parametric way to estimate the probability density function of a random variable. The aim of KDE is to find probability density function for a given dataset. In SPPA it is based on the weighted moving average of the input data, which is

$$f(u) = (1/N_b) \sum_i K[(u \text{ - } u_i)/b]$$

where

z = any location

K = kernel function (a function of distance), most commonly used is the Gaussian function [33]

b = bandwidth (how far the moving average is computed with Nb as the number of observations within the bandwidth), bandwidth equals to standard deviation.

With the help of Geographic Information System different Remote Sensing data were used to verify seasonality as for quantified burnt area, vegetation regeneration and burn severity classes. Normalized Difference Vegetation Index combined with Pixel Ident Distribution analysis was performed to assess land use change. Roads ~ trails buffer analysis was conducted to verify human activities induced fire events in dependence of road density:

(1) *Burnt area* analysis was performed in order to quantify burnt area for the period 2000-2015 to approve or disapprove the assumed dual-seasonality.

(2) *Normalized Difference Vegetation Index* (NDVI) based on selected Landsat 7 ETM+ (*date: 21.02.2000*) and Landsat 8 (*date: 28.03.2016*) was calculated in order to assess changes in land use applying **supervised classification** based on the provided vegetation map. The formula of calculating NDVI is

$$NDVI = \frac{NIR - Red}{NIR + Red}$$

where Landsat 7 ETM+ *band 4* is NIR (Near Infrared) and *band 3* is Red designated. In case of Landsat 8, *band 5* correlates NIR and *band 4* Red.

(3) *Pixel Ident Distribution (PID)*, derived from the classic spectral response pattern analysis (that is prior to any classification in order to separate different spectral response patterns in the satellite images on which the classification is based). In this study, the difference between PID and spectral response pattern analysis is that the former one is post-classification performed with the vegetation classes extracted from the Boolean vegetation map. PID was conducted for the NDVI used satellite bands, NIR and Red respectively.

(4) *Vegetation Regeneration (VegReg)* combined with *Normalized Burn Ratio (NBR)* analysis serves the purpose of detecting spatio-temporal changes in vegetation dynamism effected directly by fire and of comparing seasonal driven differences. It is based on the classic burn severity mapping, however vegetation regrowth classes enjoy priority. Mapped and assessed on MODIS verified burnt area extent. Landsat 7 ETM+ (*date: 21.02.2000*) and Landsat 8 (*date: 28.03.2016*) images were applied for the NBR calculation, thus its time scale is sixteen years. The formula for Normalized Burn Ratio driven Vegetation Regeneration analysis is

$$NBR = \frac{NIR - SWIR2}{NIR + SWIR2}$$

where Landsat 7 ETM+ *band 4* is NIR (Near Infrared) and *band 6* is SWIR2 (Short Wave Infrared 2), Landsat 8 *band 5* is NIR and *band 7* is SWIR2. What needed is

$$\Delta NBR = PreFireNBR - PostFireNBR$$

ΔNBR was multiplied by 1000, and the result was converted to integer. Classification (defining threshold values) was conducted in accordance with USGS standard [34].

(5) *Accessibility (roads ~ trails buffer)* analysis was executed to verify human accessibility of Mount Kenya Reserve and to relate roads, trails to FO (and Ignition Sources, clarified in the next chapter). The provided GIS applicable road network was expanded and many trails were drawn by the author of this thesis. Zones along (on both sides) the roads, trails were created by superimposing 0.5 and 1 km wide buffers. The resulted (buffered) roads ~ trails map was compared to reclassified FO, called Ignition Sources.

2.4. Reclassification

Reclassification was needed because of MODIS satellite detection quality. Clouds or other disturbances can cause periodic interruptions in fire detection [23], so the same fire event can be spotted in the vicinity of a previously detected one. New parameters were defined according to temporal characteristics and confidence (a scale from 0 to 100 expressed in %) of MODIS detected fire occurrences:

Ignition Classes (IC):

- **1**   - fire detected for the first time, interpreted as **Ignition Point** (**IP**)
- **2**   - fire detected on the same day or on the day after **1**, spatially close to **1**, interpreted as **After Fire 1** (**AF1**)
- **3**   - fire detected two or three days after the detection day of **1**, spatially close to **1**, interpreted as **After Fire 2** (**AF2**)
- **4**   - not identifiable, interpreted as **Unclear** (**U**)

Ignition reliability:

MODIS FO confidence range was also ordered into nine classes with 1 indicating the highest confidence level and 9 the lowest.

Ignition time:

The evidence time of detection was also evaluated and subset into nine classes as well. In this case 1 indicates the first point detected in an assumed fire event, 2 refers to the second fire point in the detection chain.
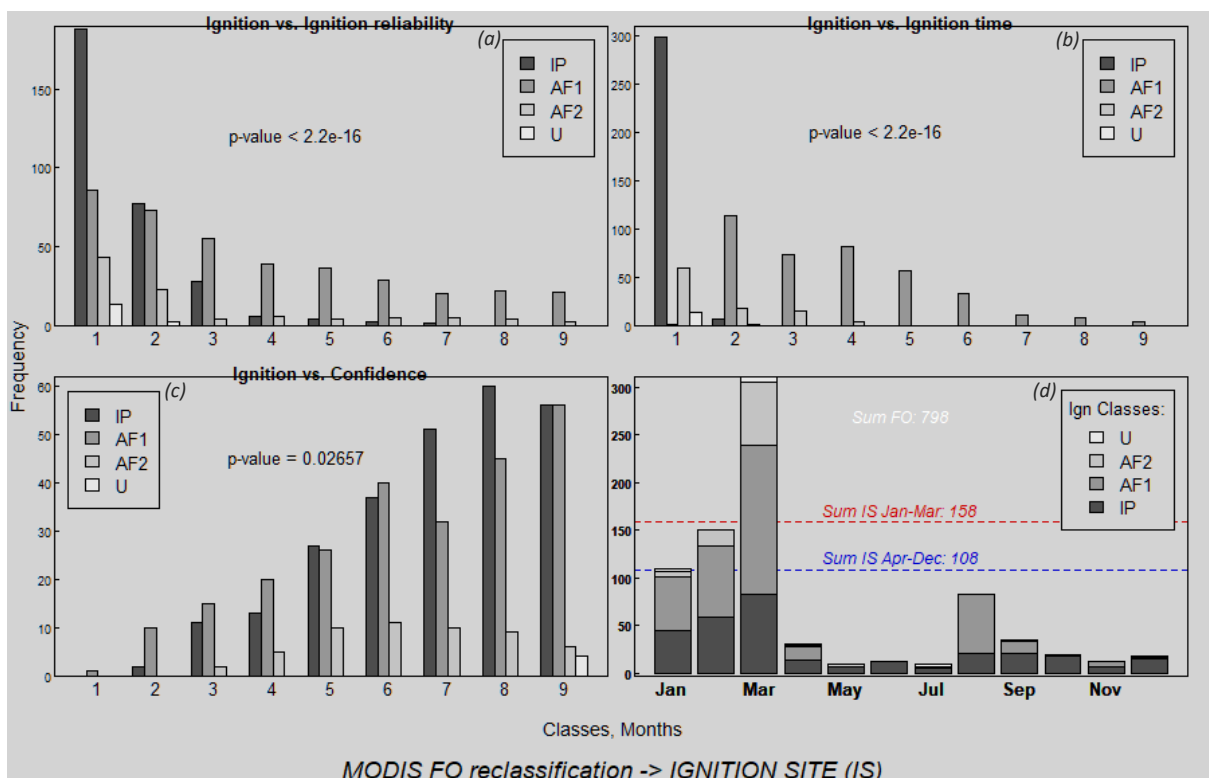
Fig. 3. MODIS FO reclassification process. Dependency between most weighted parameter and new variables: *(a)* and *(b)*, between most weighted and old parameter *(c)*. Resulted IC, denoted with gradually shading grey *(a),(b),(c)* and *(d)*. Sum of FO and IS are shown in bars *(d)*. Seasonal IS expressed with red and blue dashed lines *(d)*. P-values provided by Chi^2 tests.

10

Reclassification is defined by the new MODIS parameter set mentioned above. The weighted dependencies shown in Figure 3, between Ignition and Ignition reliability *(a)*, between Ignition and Ignition time *(b)*, and between Ignition and the old parameter MODIS Confidence *(c)* proved to be statistically significant (low p-values). Monthly FO and IC distributions are represented in bars, the Ignition Classes: IP, AF1, AF2 and U are denoted with different shades of grey *(d)*. The purpose of the reclassification process was to identify fire event **IGNITION SOURCES (IS)**. IS were finally gained by weighting **Ignition** class 1, and both **Ignition reliability** and **Ignition time** classes 1 and 2. As expected the initial number of 798 FO points was reduced to 266 IS points, 158 for January-March and 108 for April-December. In order to verify IS statistically (as a result of FO reclassification) Moran's I spatial autocorrelation (SAC) and Pearson's product-moment correlation coefficient (PPMCC) combined with SAC were executed in a comparative analysis between FO and IS.

2.5. On spatial statistics/stochastics

2.5.1. Theory: K-S, Moran's I SAC, PPMCC

First it has to be confirmed that FO spatial characteristics meet the minimum requirement for running SPPA. There cannot be complete spatial randomness (CSR) in the point data set. If there is CSR present in the data set, the author can carry on mapping and analyzing, skipping SPPA and reclassification were not needed.

Correlated variables of fire occurrences can be tested for normality using ***spatial Kolmogorov-Smirnov (K-S) test***, which examines the observed and expected distributions and in doing so it also determines how significant is the difference between them [35]. It is a powerful test of complete spatial randomness (CSR). Values of one variable are the Cartesian coordinates x or y. Values of an empirical distribution won by evaluating the function T (x, y) at each of the data points, form the predicted (expected) distribution. It means that the comparison is simply performed on the observed and expected distributions of FO x coordinates [36].

In statistical interface prediction is usually expected models are compared to measured data models on defined significance intervals. Spatial statistics has to deal with spatial and temporal object such as points and polygoned areas. As far as reclassification concerned, additional explanation is needed. The point is that on purpose defined statistics of the present thesis go against the usual basic laws of statistics, and the concepts of reclassification were formed accordingly. Moran's I spatial autocorrelation and Pearson's product-moment correlation coefficient tests were run to prove **non-dependency** of IS points.

Moran's I spatial autocorrelation (SAC) measures similarity between close objects in comparison with other close objects [37, 38] in a spatial field. It can be classified as positive, no or negative spatial autocorrelation and takes values from -1 to +1.

- In case of positive spatial autocorrelation similar values cluster together in a given area, can takes values between **+1** and **0** where values closer to +1 represent strong positive autocorrelation.
- Negative spatial autocorrelation is when dissimilar values cluster together in a given area, takes values from **0** and **-1**. The closer to -1 the stronger negative autocorrelation is.
- No spatial autocorrelation means that observed objects are independent and they are **0**, which is very rare, most of the time they are very close to or around zero.

Clustering, close by points with similar autocorrelation values might be part of the same fire event (see previous section on *Ignition*, *Ignition reliability* and *Ignition time*) so they are assumed to be the same fire event. Ignition Sources (IS) points are considered as the ignition sources of fire events, numbering fire events. If these fire events (IS) show no spatial autocorrelation, taking close values around zero, their differentiation from each other is confirmed. With other words, they are spatially-temporally independent fire events.

Pearson's product-moment correlation coefficient (PPMCC) is a widely-used statistic method in all kind of science. It measures the strength of linear correlation between two variables. Range of values is set between +1 and −1 inclusive, where:

- **+1** implies a perfect positive association between the variables meaning if values go up on one, they also go up on the other
- **-1** implies perfect negative association between variables meaning if values go up on one, they go down on the other
- **0** implies no linear association.

The variables were on one side the FO and IP points, and on the other their nearest neighbor (NTH) fire points [39]. For visualization smoothed trend fit lines were applied to the graphs.

Aiming at no correlation, the PPMCC test was run to verify the results of reclassification process more pronounced than it was done by Moran's I SAC. Fire points, FO and IP, are compared to their 1st, 2nd, 3rd,… xth NTH nearest neighbour and computed for linearity. Hence their values are the same, PPMCC values are interpreted for Moran's I spatial autocorrelation.

2.5.2. Implementation: K-S

Null-hypothesis behind the spatial Kolmogorov-Smirnov test, illustrated in Figure 4 is that there is no difference between observed and expected distributions of FO x- and y-
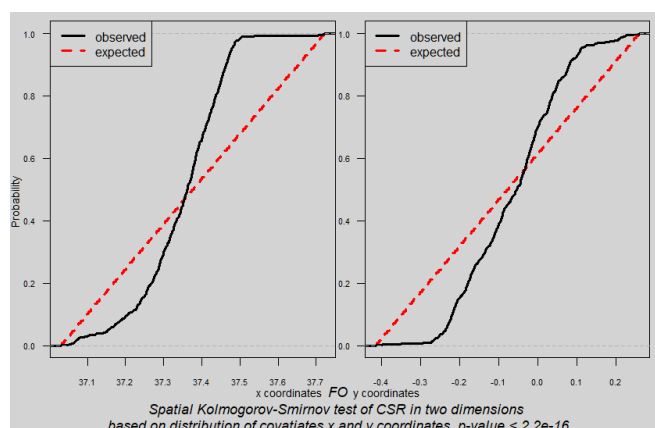
Fig. 4. Spatial Kolmogorov-Smirnov test for testing MODIS detected fire occurrences (FO) for complete spatial randomness (CSR).

coordinates obtaining CSR in this case. P-value smaller than $2.2*10^{-16}$ provided by the K-S test suggests enough evidence to reject the null-hypothesis. There is difference between observed and expected values. With other words: no CSR is present! Spatial point pattern analysis can be thus conducted.

2.6. On thesis procedure

The build-up of this thesis followed an analysis-response interaction line (Fig. 5.): a performed analysis (in circle) always had a response, conclusive results (by triangles symbolized) that paved the way for a further analysis. This also had conclusive results guiding into the next analysis. The response of one performed analysis was the conclusive result leading into another analysis stimulated by the results (of the former analysis). This phenomenon has made the study flow along an analysis-response interaction line. The logic-analytical responses FO reclassification, Discussion and conclusions, Recommendations performed by the author are depicted by ovals. The connection between VegReg and Burnt Area analysis shows that VegReg was conducted on the extent of MODIS verified burnt area.

Obviously, as shown by Figure 5, the results of SPPA triggered *FO reclassification* which resulted in IC. Once ignition classes and IS existed, spatial statistical analyses were run to check whether the aimed ignition sources spatial non-dependency of ignition sources is achieved or not.

All other RS-GIS analyses Burnt Area, NDVI, VegReg and roads ~ trails Buffer were conducted afterwards, their results building the pedestal on which *Discussion and conclusions* lays. *Recommendations* include *general recommendations*, and *particular recommendations* providing GIS-ameliorated data which is very promising regarding future forest fire management and further researches at Mount Kenya.
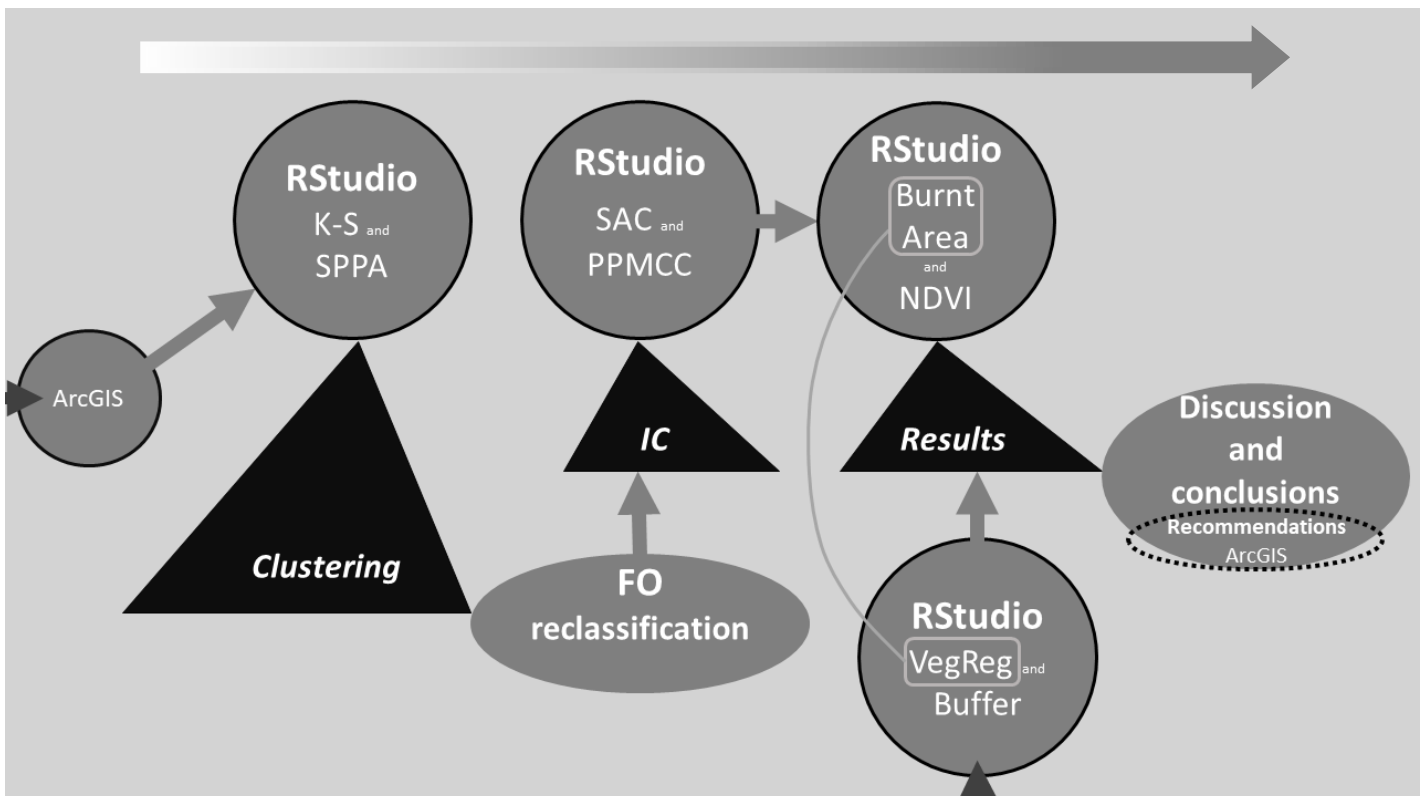
Fig. 5. Simplified visualisation of thesis evolution process. Circles contain analyses, triangles express results and logical-analytical responses of the author are in ovals. Dark grey arrow heads mark initial phases and a timeline is represented by the arrow above. Dotted oval indicates that recommendations are treated as a separate chapter.

3. Results

3.1. Seasonality

The MODIS detected FO, depicted by Figure 6, follow a spatially random distribution pattern with local aggregations, clustering. The seven FO frequency classes reveal that about two-third of FO that belong to high frequency classes (Class 4, 5 and 6) contribute to a shorter
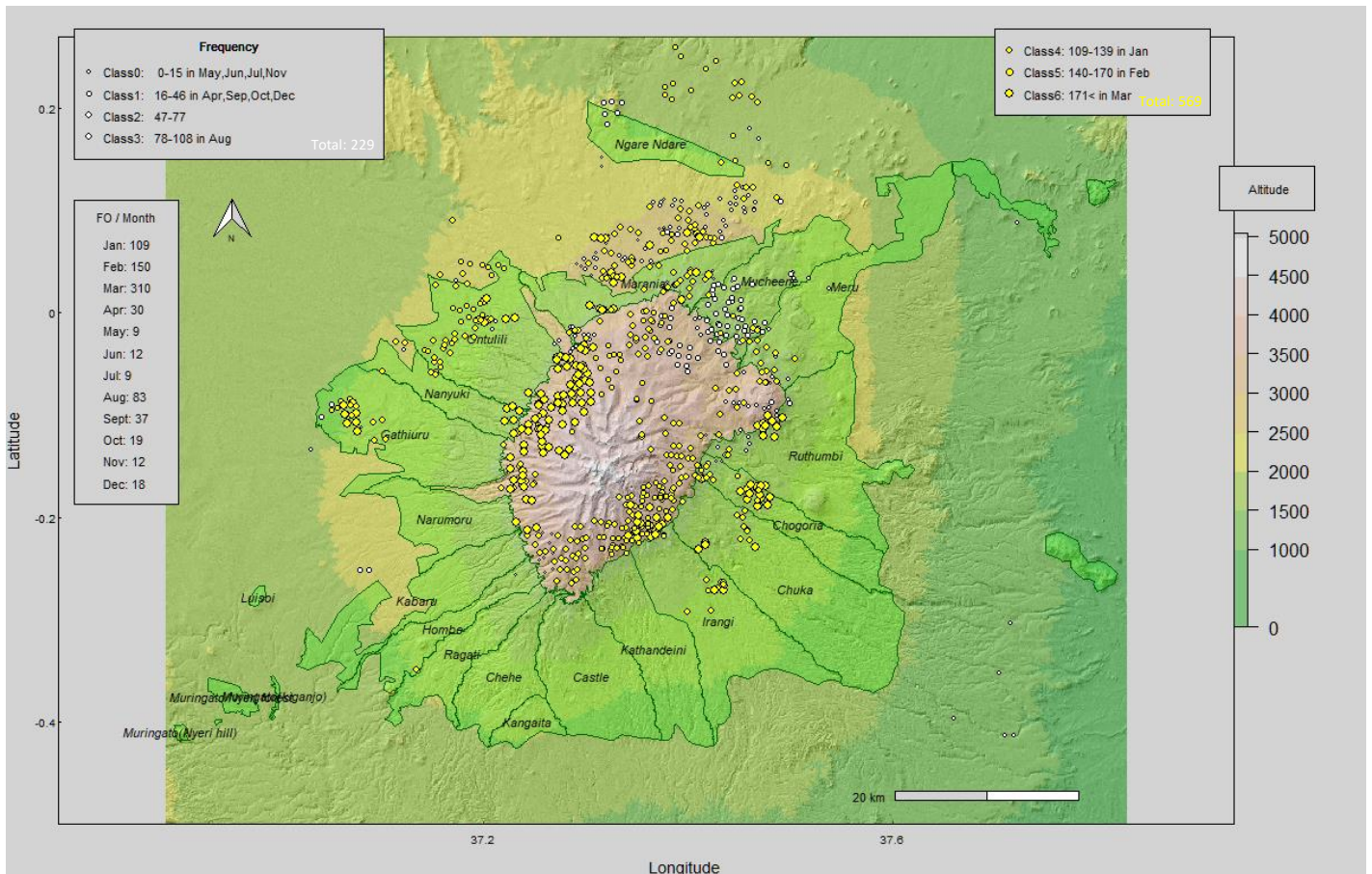
Fig. 6. Spatial distribution of FO frequency classes. Bimodal seasonality expressed by white and yellow dots. Forest station names displayed.

period of the year, namely January, February and March. The precise ratio is 229 to 569, where the smaller sum of FO is distributed over the long period of year, from April to December. It is clearly visible that the fire frequency distribution highlights fire regime's dual seasonal characteristic with March and August as peak months in the Mount Kenya region.

Remarkably, the majority of FO are detected outside the forest stations, on the high altitudinal moorland and on the area in the North above Marania forest station.

Further analyses are executed within the scope of this dual seasonality: January-March and April-December, distinguished as **high** and **low** (fire) season, or **fire-prone** and **non-fire prone** season, respectively.

3.2. SPPA

3.2.1. Variance to Mean Ratio

The April-December FO density raster (Fig. 7.) shows clustering FO behaviour. Quadrats with zero FO counts are not visualized. The histogram of fire density distribution, however, includes quadrats with zero FO counts. With 4.31 VMR value spatial clustering pattern is highlighted. The mean FO pro quadrat is 4.75.

Figure 8 reveals with mean 8.54 FO pro quadrat clustering characteristic as well. White empty dots indicate number of FO and their relevant quadrat counts. The further VMR from
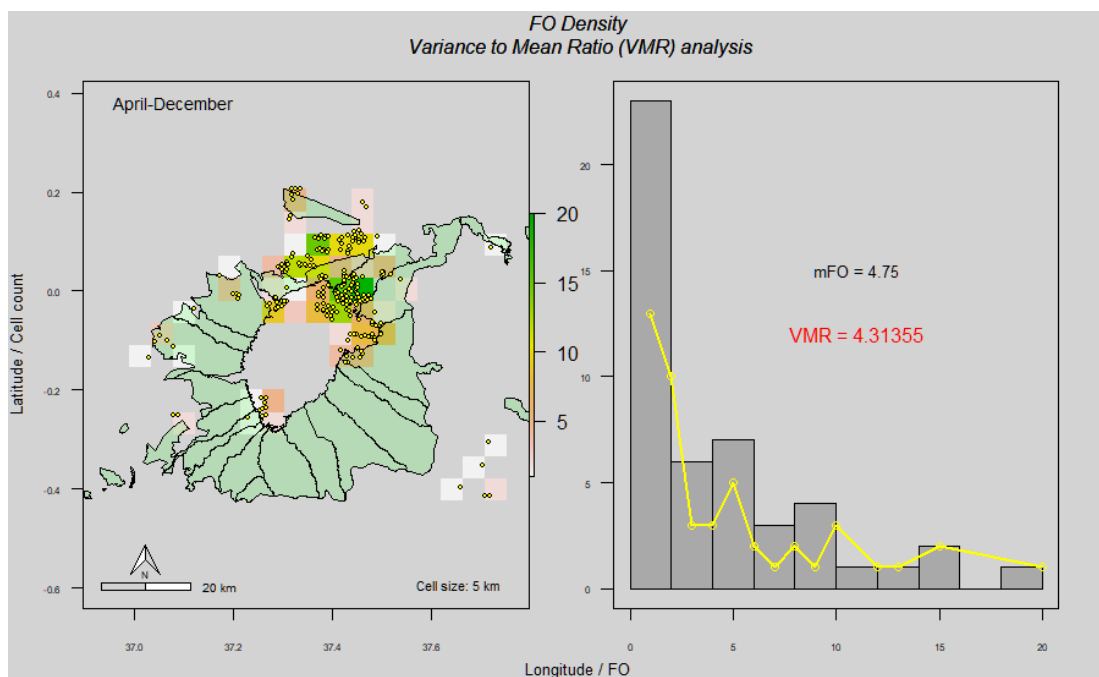
Fig. 7. Spatial FO density distribution and the results of VMR for low fire season. Yellow empty dots indicate FO sums of spatial corresponding quadrats.
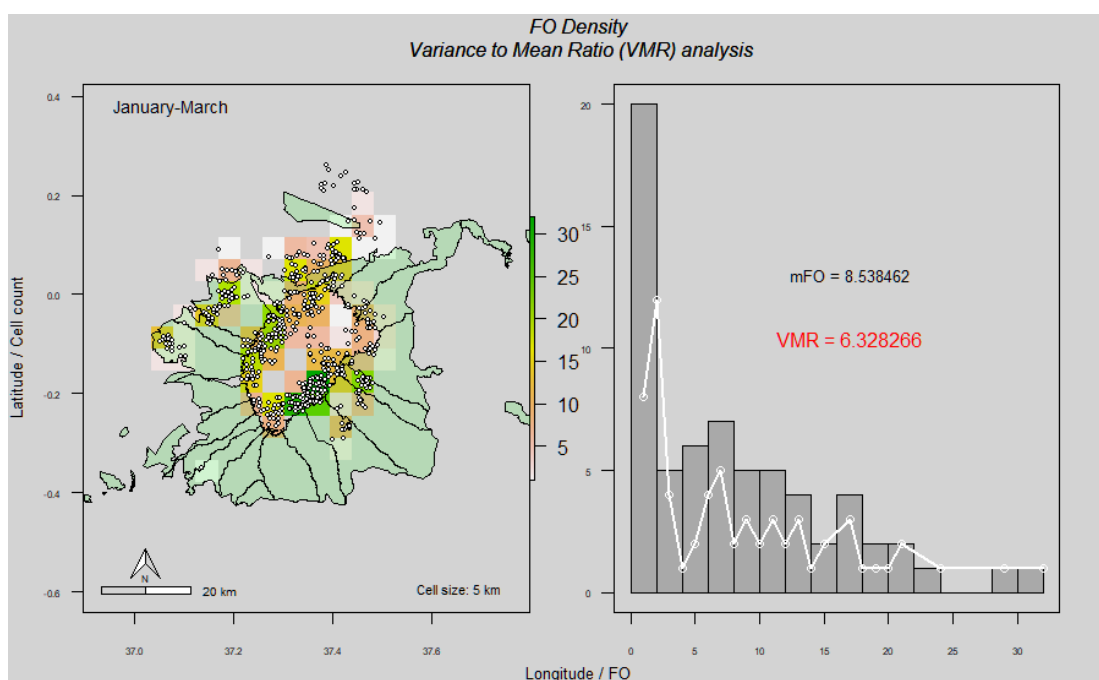
Fig. 8. Spatial FO density distribution and the results of VMR for high fire season. White empty dots indicate FO sums of spatial corresponding quadrats.

the value 1 is, the more intensified indicated spatial clustering is. With a VMR value of 6.328266 becomes FO clustering behaviour more pronounced.

The January-March period shows a near double mean fire occurrence density (mFO) and a relative denser FO clustering (2.015 higher VMR value) in comparison to the low fire season. The difference between the highest numbers of FO pro quadrat are also notable. 20 for the April-December period, whereas 33 for the high fire season.

3.2.2. G-function

Results of the nearest neighbour distance with MMD for both FO seasons can be examined in Figure 9. The estimates of the nearest neighbour distance are: Kaplan-Meier, border corrected, Hanisch and Poisson for complete spatial randomness (CSR). For the sake of interpretation, it is sufficient to look at values of various estimates of the nearest neighbour function $G(r)$ and compare them to the values of Poisson's (equivalent to CSR) $G_{pois}(r)$. Obviously, all three: the Kaplan-Meier, the border corrected and the Hanisch estimates overlap each other, having the same values. If the nearest neighbour distance in the point pattern is shorter than Poisson $G(r) < G_{pois}(r)$, it suggests clustering in the point pattern. In case of the function values, there is smoothening to be observed at a distance between 10-20 m, marking the threshold between regularity and clustering for the FO point pattern. Indeed, the steep increasing lines of nearest neighbour distances are almost flat at 12 m distance for both seasons. Clustering pattern at short distances is observed for both seasons independently from seasonality.
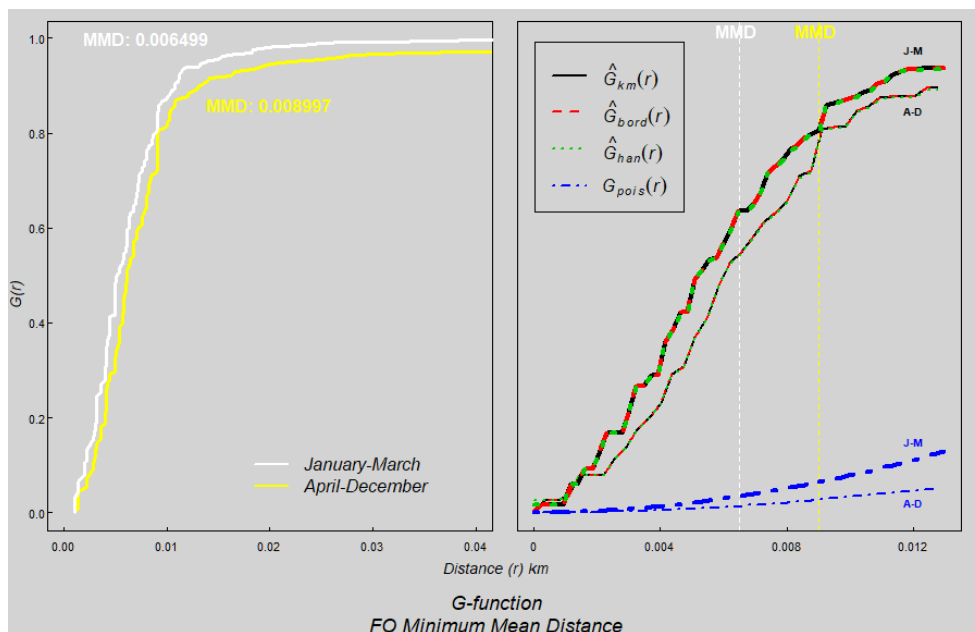
Fig. 9. G-function, FO nearest neighbour distance with Minimum Mean Distance (MMD) for high and low fire seasons.

These results suggest that MODIS detected FO are likely to occur on the same location in the period between 2001 and 2015.

Clustering nature of the G-function are surprisingly only useful for very short distances due to FO point pattern characteristics. Therefore, the needs of implementing other scaling up distance method were met.

3.2.3. Ripley's K-function

The K-function, by comparing estimates of *K(r)* to K_{pois} *(r)* (equivalent to CSR) directly reveals clustering or regularity. The choice of estimator does not seem to be very important as long as there is edge correction applied [27], which is automated in RStudio's computational
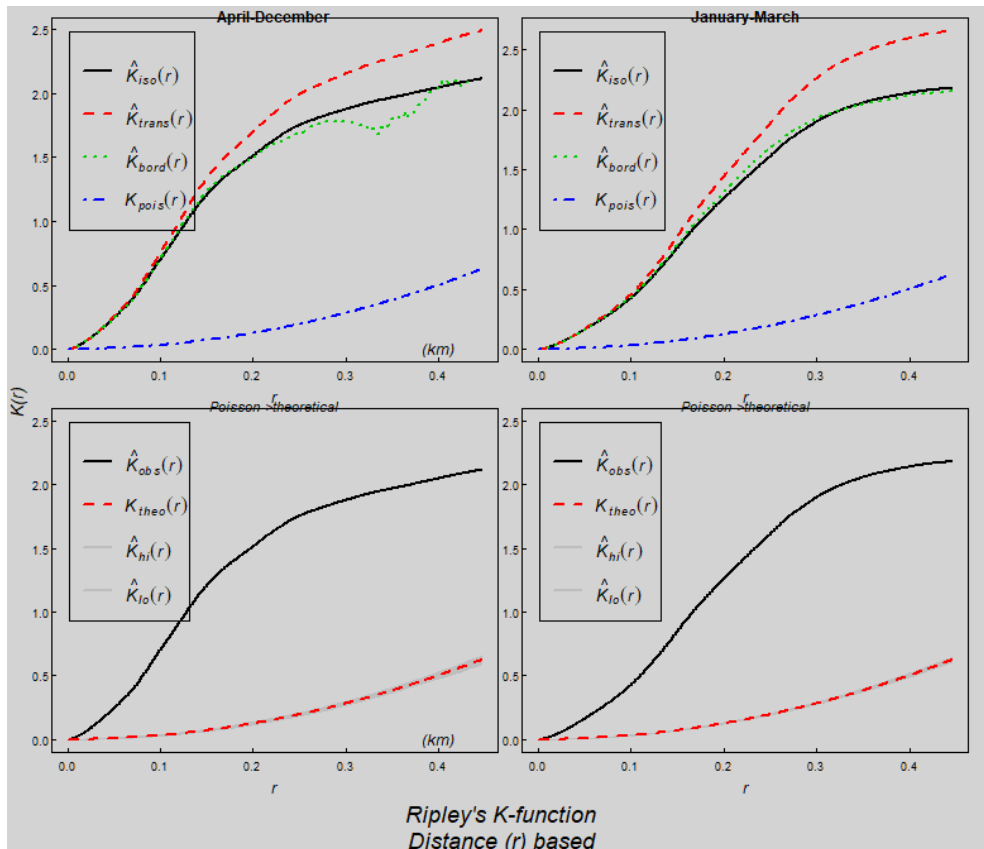
Fig. 10. FO Ripley's K-function analysis. Top: true K(r) estimates for both seasons. Bottom: simplified K(r) estimates for both seasons.

environment. Values *K(r)* > K_{pois} *(r)* suggest clustering, while *K(r)* < K_{pois} *(r)* imply at regularity in a given point pattern.

Top graphs of Figure 10 show the K(r) estimates: Ripley's isotropic correction - black solid line, translation corrected - red dashed line, border corrected - dotted green line and the theoretical Poisson, represented by dot-dashed blue line for CSR.

Bottom graphs of Figure 10 visualize a simplified K(r) estimate approach, where red dashed lined K_{theo}(r) is Poisson, black solid lined K_{obs}(r) corresponds to Ripley's isotropic correction estimate. Theoretical highest and lowest values are also computed, represented with grey lines, showing insignificance.

Estimates of *K(r)* for both seasons show steep deviation from Poisson, clearly

suggesting clustered characteristics in FO point pattern. The April-December line is up to 250 m strongly pronounced, the same characteristic appeal up to approximately 350 m to the high fire season line. The observed FO clustering are in both seasons obviously smoothed at the end of their shown distance scale, at around 350-400 m

3.2.4. Kernel Density
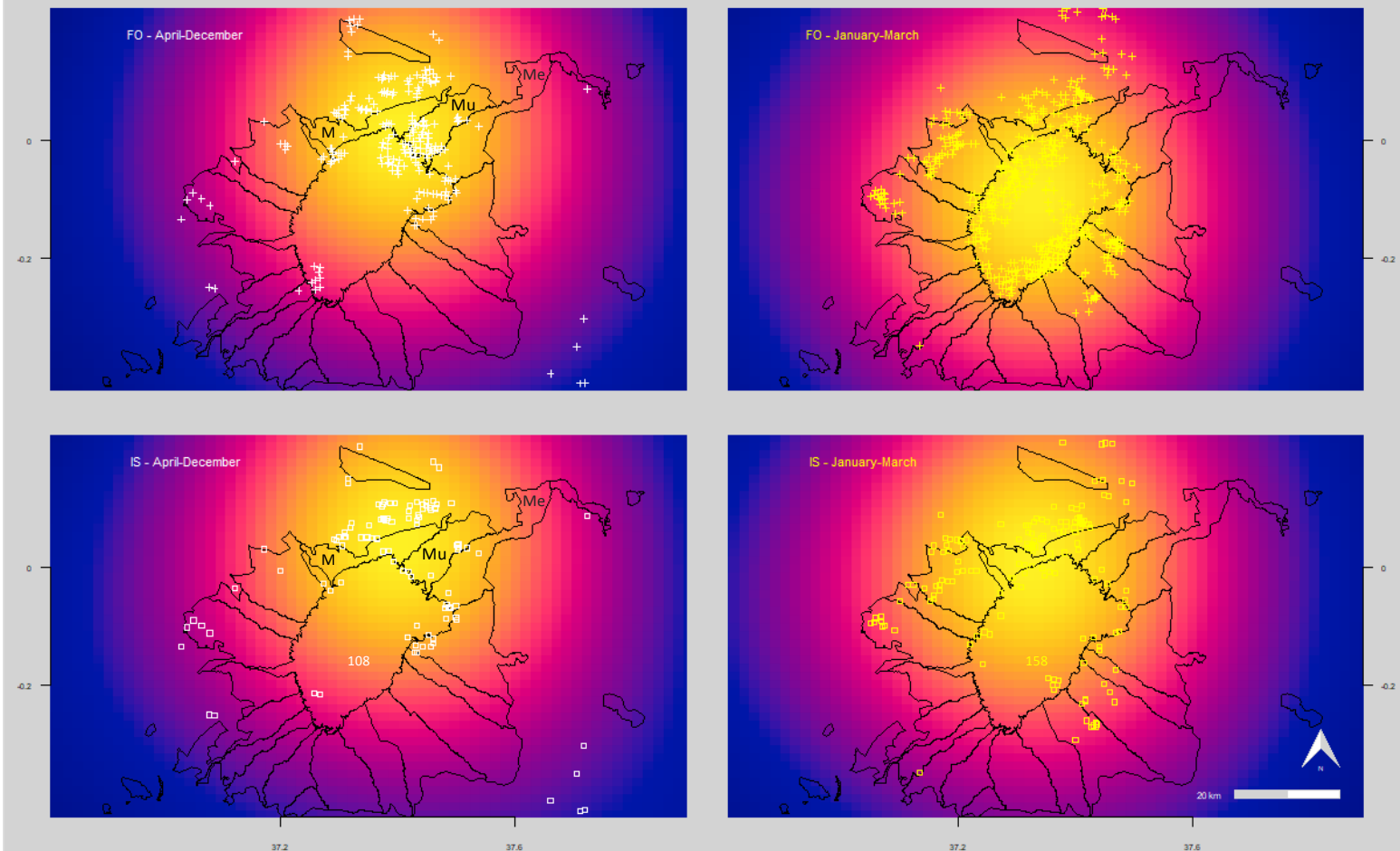
Fig. 11. Kernel density comparative maps for both FO and IS as to bimodal seasonality. Low to high density expressed with brightening colour palette, from blue to orange. M is Marania, Mu refers to Mucheene and Me to Meru forest station.

Surprising results brought by the Kernel Density Estimate comparison between FO and IS can be viewed in Figure 11. Low seasonal MODIS detected FO aggregate in the northern part of Mount Kenya, concentrated in Marania, Meru and especially in Mucheene forest stations and in their vicinities. Density centre can be identified at the intersecting point where the upper boundary lines of Marania and Mucheene meet. IS number less points within the forest stations noted (with Mucheene encompassing most FO) and becomes more weighted on the cultivated fields outside the low altitudinal boundary of Marania. Accordingly, a slight

shift of density centre is to be observed towards the North. So, the IS kernel density centre is located in Marania. This, spatially seen, is an insignificant change.

January-March FO kernel density centre is on higher altitude. Viewed from the map's geographical centre, it is located between the moorland and the Kenya massif, a bit to the north. Comparing to the IS map, a significant shift of density centre can be observed. The density centre 'moved' to the North, directly towards Marania forest station and is established there. As far as the upper area (above the high altitudinal boundaries of forest stations) concerned, the 'drastic' reduction of FO resulted in 29 IS adjacent to the forest stations. Indeed, IS on high altitude are concentrated nearby the upper boundaries of surrounding forest stations.

IS centres for both seasons are very similar, spatially almost overlapping each other.

3.2.5. Statistics: Moran's I SAC, PPMCC

- Moran's I spatial autocorrelation (SAC)
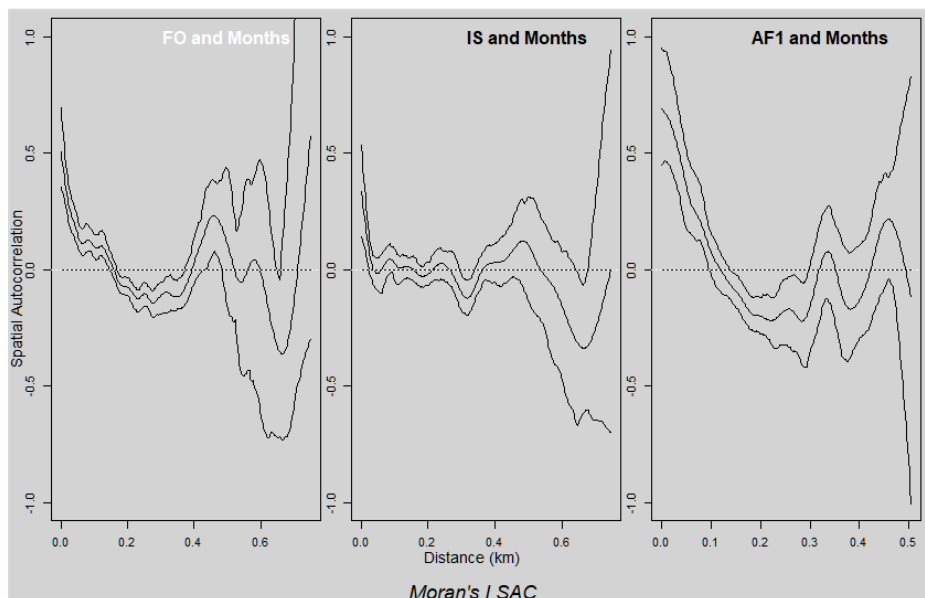
Fig. 12. Moran's I Spatial Autocorrelation test comparing IS and AF1 to FO for spatial dependency. Distance unit in km, while autocorrelation is unitless.

Described in section 2.2.1., reclassification's aim was to reduce spatial autocorrelation between fire points, expecting IS autocorrelation values close to zero.

As shown in Figure 12, according to the weighting of points: FO, IS and ignition class AF1 by the independent variable *Months*, one of MODIS detected FO parameters, autocorrelated values vary. Comparison between FO and IS need to be considered particularly. The initial negatively and positively autocorrelated FO values became smoother at distances up to 350-400 m: IS values run along the zero line. Furthermore, the test unveils the AF

characteristics. Points of AF1 are the pulling agents of the original data set, making FO autocorrelation point values either positive or negative.

- Pearson's product-moment correlation coefficient (PPMCC)

Figure 13 confirms the expectation that FO and IP (thus IS) have different neighbourhood relation and have to perform differently under the PPMCC test. Although the MODIS detected FO points trend line (blue) glides smoothly downward from weakly positive to weakly negative correlations, the red IP trend line runs nicely along the zero and is therefore a much better fit. It means that linear association between Ignition Sources are minimised making fire events more independent.
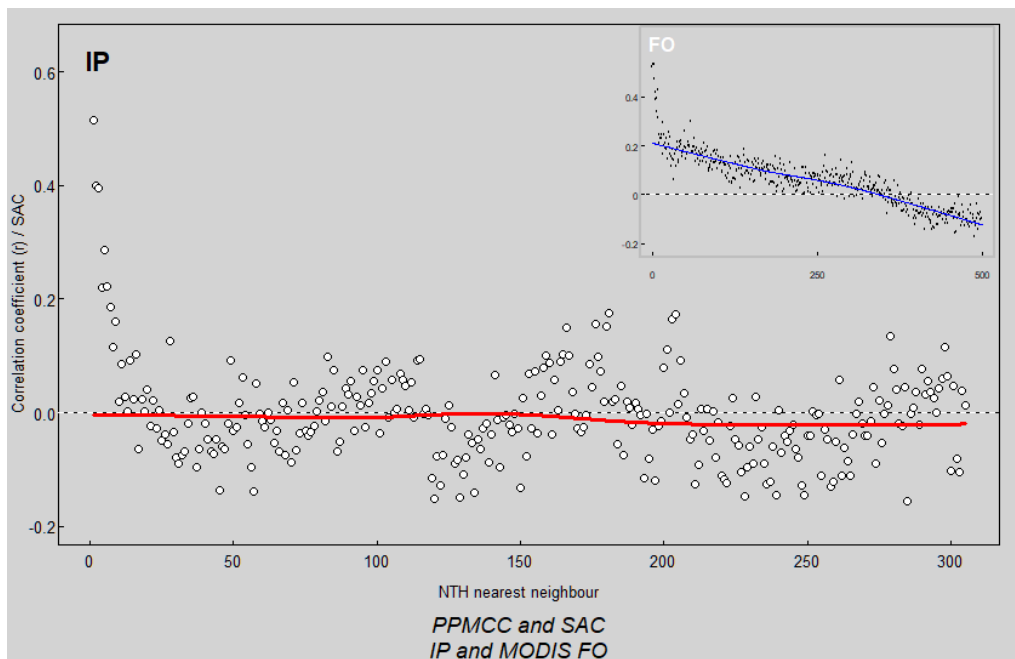
Fig. 13. PPMCC test of IP and FO (inset graph) for linear correlation (expressed by smoothed trend lines) and SAC.

3.3. RS - GIS

3.3.1. Burnt area

Figure 14 emphasises the dual seasonal fire characteristics with peaks in August for April-December, and in February for January-March. In the fire-prone season 41677 ha area was burnt from 2001 to 2015. This is more than double than the summed size (17537 ha) of low seasonal burnt area.
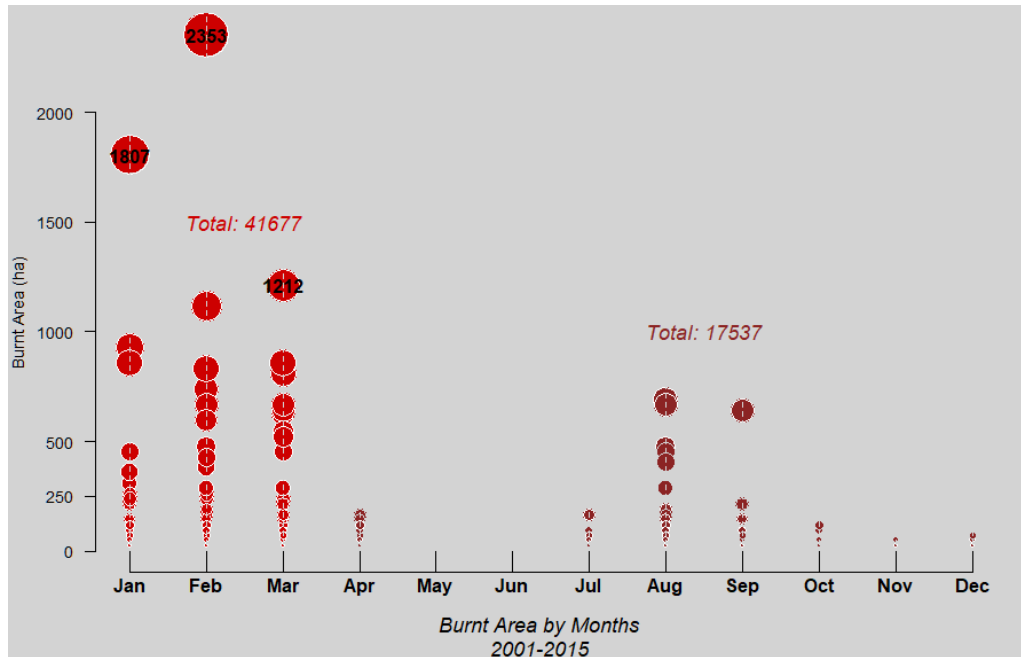
Fig. 14. Monthly distribution of area burnt. Fire seasonal differentiation indicated by red and brown colours. Increasing bubble sizes express burnt area sizes. Unit in hectares.

The most complex analysis of the thesis at hand was depicting MODIS burnt area data in time series with respect to dual seasonality. Selection was based firstly on location, secondly on sizes of burnt areas.

Three remarkable years, in which more than 1500 ha area was burnt (Fig. 15.), can be highlighted for the non-fire-prone season. The years of 2002, 2008 and 2014, respectively. Not surprisingly, it is August when the largest areas were burnt. The summer of 2008 was unexpectedly hot in terms of fire activity, because there was 8805 ha partly forest and partly moorland vegetation burning. It means almost ten times more burnt area during this summer in comparison to the median, 943 ha burnt area for the selected fire years.

Concerning fire-prone season (Fig. 16.), six years can be selected when more than 1500 ha area was burnt, namely 2006, 2009, 2011, 2012, 2013 and 2015. Peaking with 12171 ha the year 2012 happened to be the most devastating (more than two times bigger burnt area than in 2009 when 'only' 5579 ha was burnt) fire year during the studied period. The median burnt area is 1643,5 ha, which is less than six times smaller than the burnt area size of the top year recently described.

High seasonal burnt area suggests fire events burning bigger areas, whereas low seasonal fire events burn in general smaller areas.
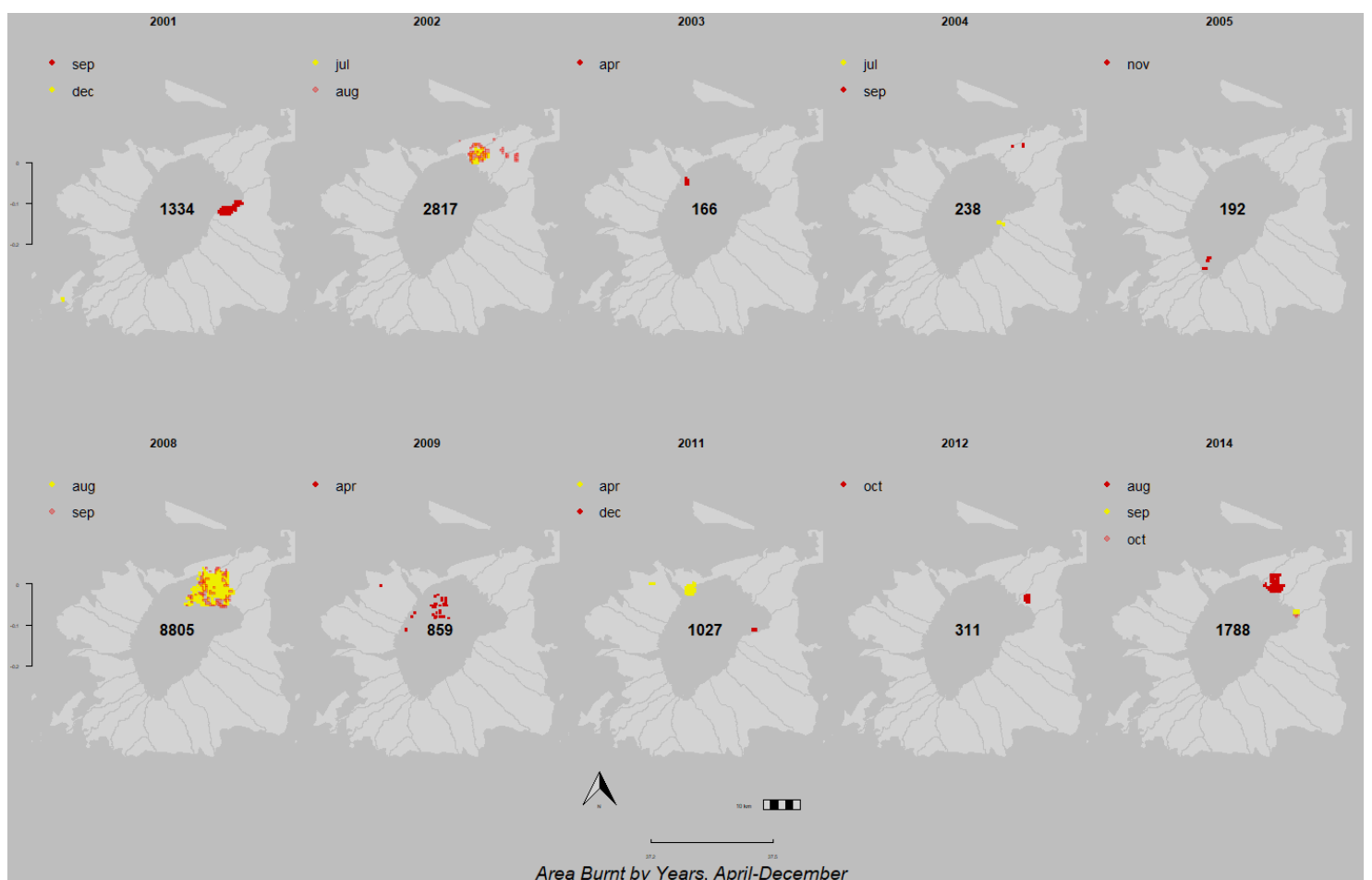
Fig. 15. April-December burnt area time series in Mount Kenya region. Numbers in the middle indicate hectares burnt by year. Red, yellow and light red colours represent burnt areas by relevant months between April and December.
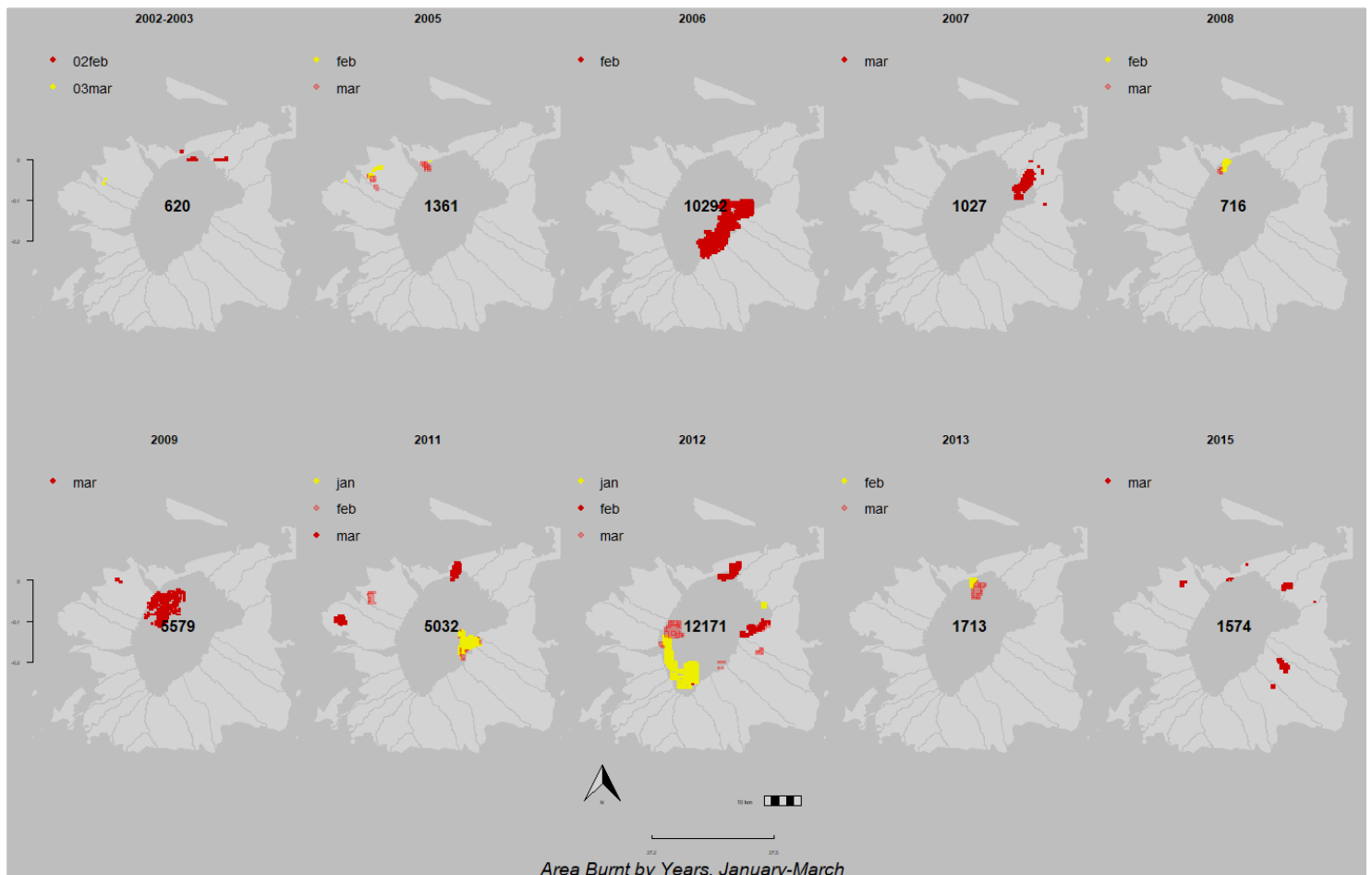
Fig. 16. January-March burnt area time series in Mount Kenya region. Numbers in the middle indicate hectares burnt by year. Red, yellow and light red colours represent burnt areas by January, February, or March.

22

As shown by Figure 17 (where IS and AF 1 imitate direct 'on the day of ignition and day after' fire spread), the combination of IS with AF1 covers the burnt area quite fittingly. From a spatial point of view, Some AF 1 could possibly be identified for spatial upscaling to IS.

There are proportionally more IS to be observed within the forest station boundaries than on the moorland. In case of North of Marania, where the accumulation of agricultural land is dominant, lot of IS are present with no burnt area coverage. These must have been small fire events with no or very short distanced (by satellite not detectable) fire spreads, or false alarms.

More frequent but smaller fire events are thus more likely to occur within the forest stations, while less frequent but larger fire events are more likely to happen on the moorland. In addition to it, forest stations have to deal with more frequent fire events during the fire prone season.
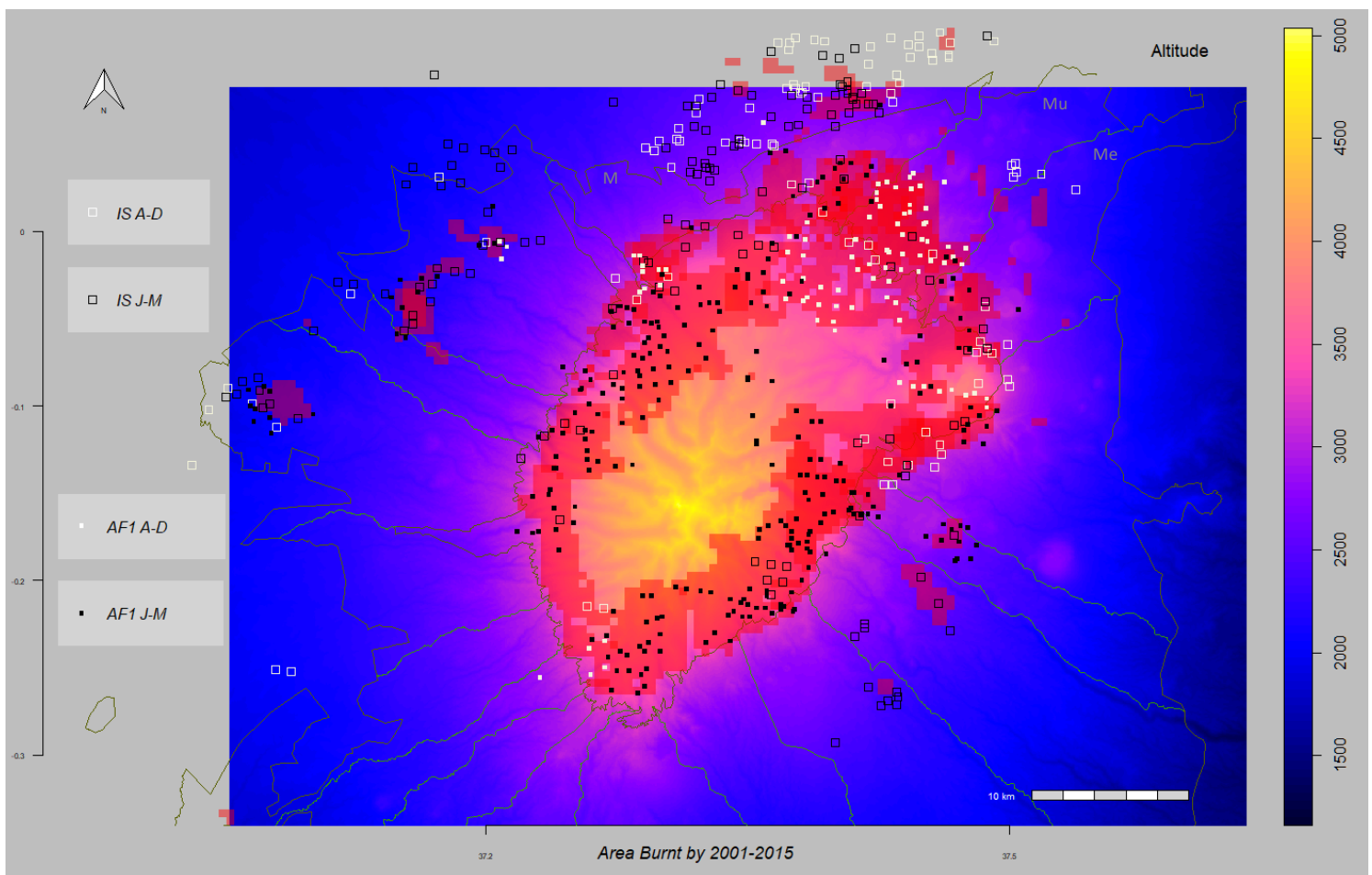
Fig. 17. MODIS verified 500-m burnt area. IS and AF1 displayed regarding dual seasonality. M is for Marania, Mu refers to Mucheene and Me to Meru forest station.

According to MODIS verified burnt area product, these fire events burn more forests (within forest station boundaries) than low seasonal fire events do (Fig. 18.). The observed differences regarding burnt area distribution between high and low seasons are in size and spatial location. As expected, dry seasonal burnings are concentrated by far on the moorland.
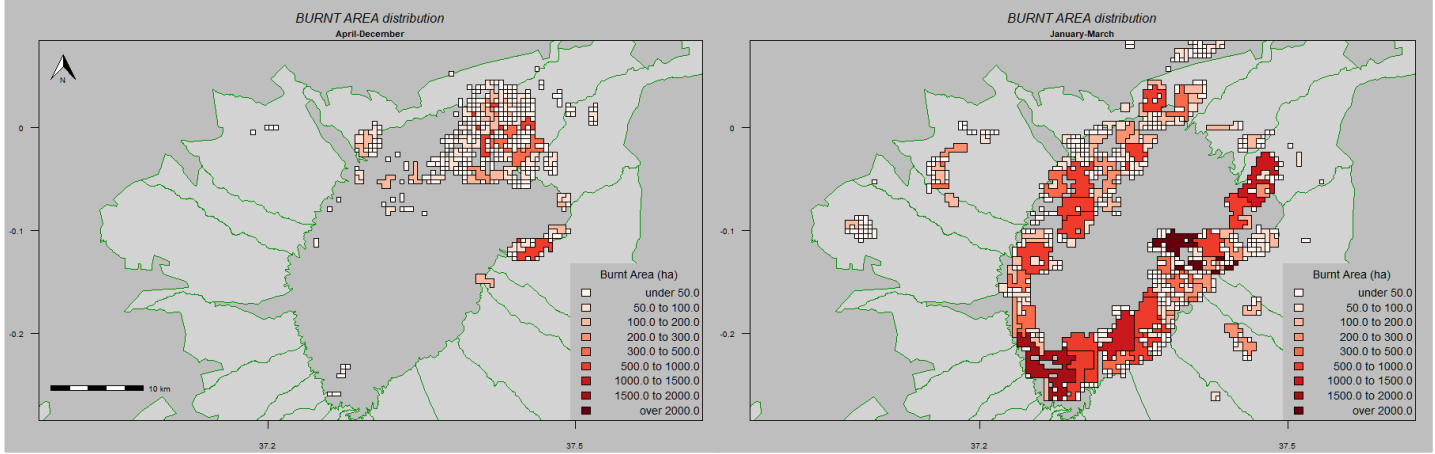
Fig. 18. MODIS verified burnt area size distribution displayed for both seasons. Unit in hectares.

Furthermore, within the forest stations the vast majority of burnt areas are small sized, averaged between 100-300 ha while on the moorland three-four-five times bigger burnt areas dominate.

3.3.2. NDVI and PID

Samplings for the NDVI supervised classification are based on the classified Boolean Mount Kenya vegetation map (introduced in chapter 2.2.1.). The classification itself was performed on a 'to the rectangular extent of forest stations' clipped version of calculated NDVI year 2000 image displayed as a black frame in Figure 19, because unlike the 2016 image, it was cloudless over the Kenya massive. Sample plots are also visible.
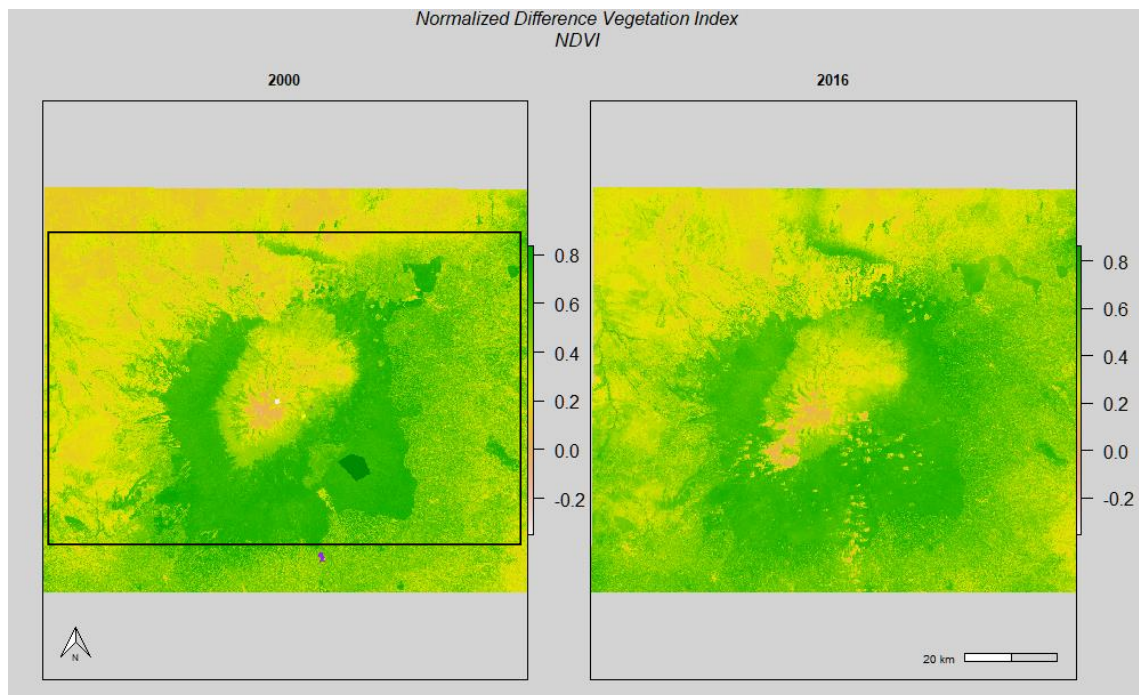
Fig. 19. Calculated NDVI images used for supervised classification on the extent shown by black frame.

NDVI pixel distribution unveils a prominent shifting towards higher values (Fig. 20.). A general change in vegetation distribution is to be observed, irrespectively to the bimodal seasonality. Values between 0.2 and 0.5 (grass, shrub, crop) are most probable and clearly decreasing.

24
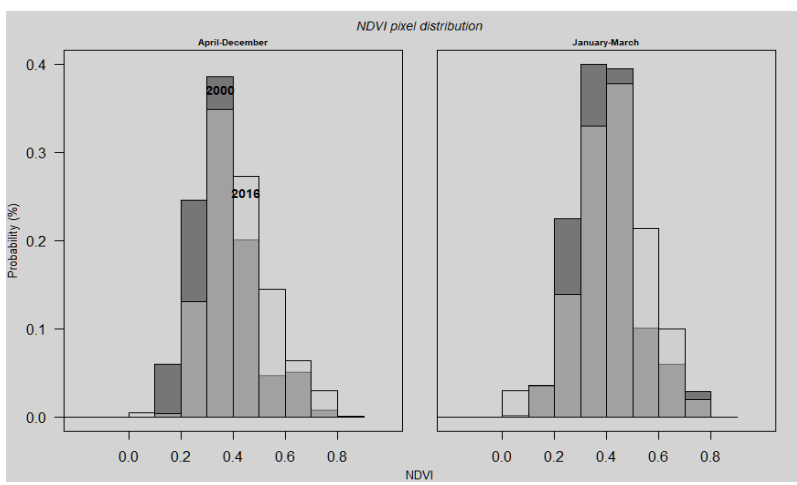
Fig. 20. Comparative NDVI probability pixel distribution. Year 2000 expressed by dark grey, year 2016 by light grey bars. Overlap is greyed. NDVI is unitless.

NDVI values from 0.6 however, are increasing in a relative comparison to cropland values gaining more weight. In general, vegetation is more productive (higher assimilation) in fire prone season, suggesting connection to fire. To gain more insight in this topic, further researches are needed.

Remote sensing data based Pixel Ident Distribution (Fig. 21.) show for the NDVI 2000 image a point pattern with differentiated clustering behaviour, forest (NDVI values 0.6-0.8) and cropland pixels are slightly overlapping in each other NDVI value range 0.6-0.7. A totally different point (pixel) pattern can be observed for the NDVI 2016 image (Fig. 22.). Here, besides a stronger clustering pattern observed for all vegetation types, more pronounced overlapping, with/within each other structured layering can be perceived for the five vegetation classes. This phenomenon is strongest between the moorland and the otherland.
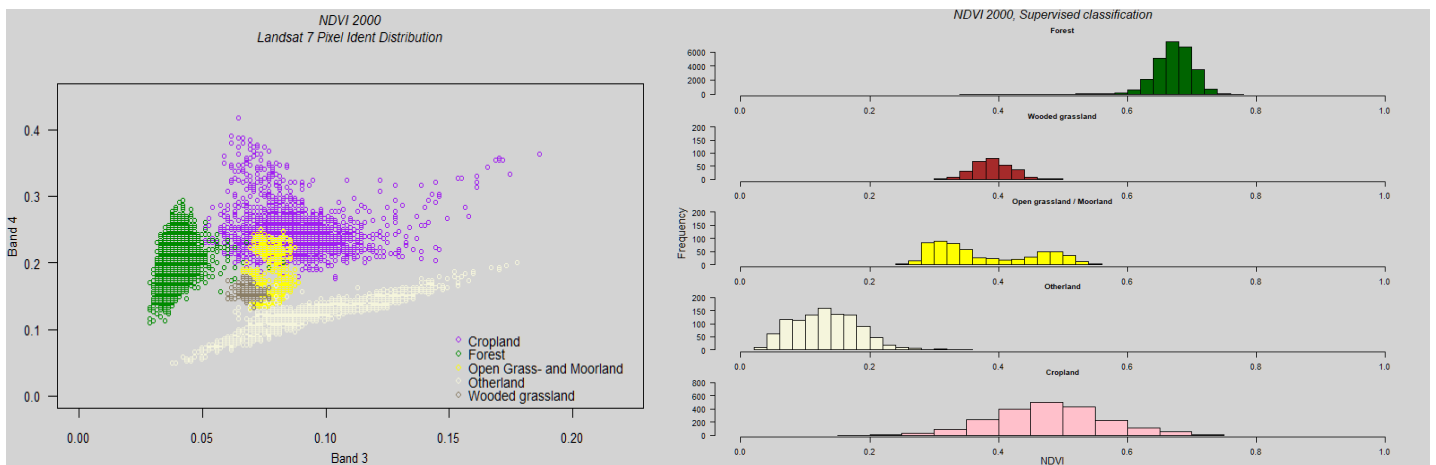
Fig. 21. Pixel Ident Distribution of for 'NDVI 2000 based supervised classification used bands' (left), presenting vegetation classes pixels. Supervised classification (right), vegetation classes distribution over NDVI.
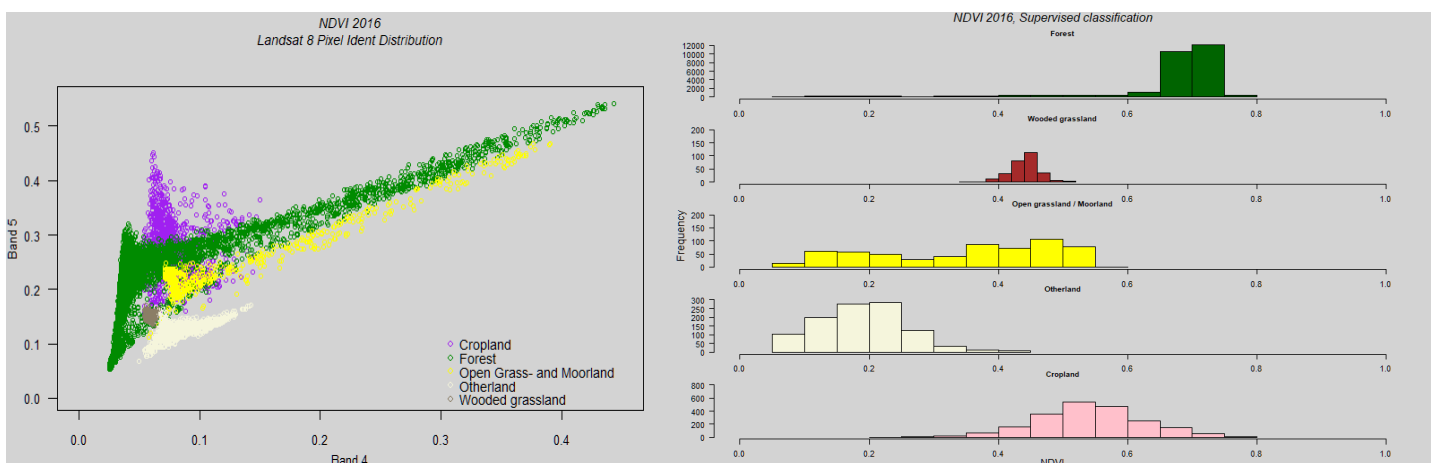
Fig. 22. Pixel Ident Distribution of for 'NDVI 2016 based supervised classification used bands' (left), presenting vegetation classes pixels. Supervised classification (right), vegetation classes distribution over NDVI.

3.3.3. Vegetation Regeneration and Burn Severity
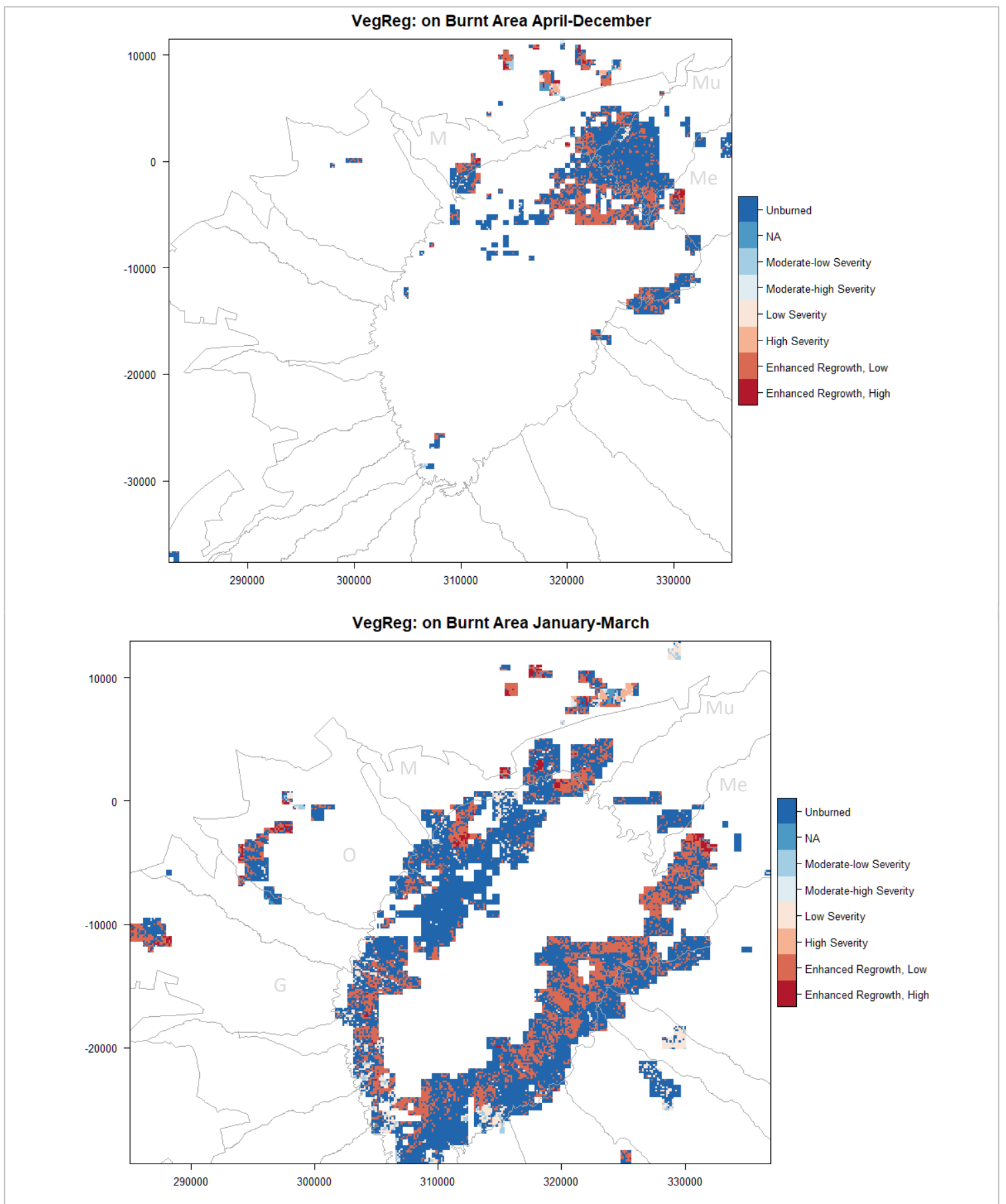
Fig. 23. Vegetation regeneration dynamic and burn severity assessed on burnt area for April-December (top) and for January-March (bottom), derived from ΔNBR. Burn severity classes, Enhanced Regrowth Low (red) and High (dark red) are expressed with intensity colour palette. NA meaning no pixel value. Forest stations from links: Gathiuru, Ontulili, Marania, Mucheene and Meru.

The classes determined for the analysis are quantitatively interpreted based on ΔNBR (section 2.3.2). Here, Enhanced Regrowth Low, equivalent to regeneration and Enhanced Regrowth High, or advanced almost grown vegetation are in focus. Because of the rapid natural regeneration (Nyongesa, verbal comment), the former indicates recent (several months in the past) fire events, while the latter suggests fire events that occurred around a year or years before. In science burn severity is always classified according to quantified loss of organic material either aboveground or in the soil or water, depending on the purpose of research [41].

Figure 23 shows North of Marania (M) as a catalytical centre where the most High Severity pixels can be seen. This piece of landscape is driven by constant human activities throughout the year, as it fosters Moderate-low Severity, Moderate-high Severity, Enhanced Regrowth Low (equivalent to regeneration) and High classes, irrespective of which season they occur in.

While scanning through the 'by fires of non-fire prone season burnt' forest stations, their landscape shows less fire activity in comparison to North of Marania. Still, as the case of the most affected forest station Mucheene (Mu) shows: Enhanced Regrowth Low, although its spread is spatially scattered, is constantly to be spotted. In Meru (Me) forest station the presence of Enhanced Regrowth High surrounded by regenerating vegetation is a sign of fire driven landscape. On the moorland, as expected, regrowth (Enhanced Regrowth Low particularly) pixel frequency proportional to burnt area size of the season is increasing, suggesting more intense fire activity than in the forest stations (exclusive Meru).

Considering only the classes of burn severity index (without the two regrowth classes) of the fire-prone season, the forest is shaped by less intense fire events with burn severity pixels of Moderate-low, Low and High spotted here and there. By including the two regrowth classes into the analysis, the picture of a dynamic changing landscape, shaped by fire, is unveiled. The forest station Ontulili presents a wide range of burn severity and both vegetation regeneration classes: Moderate-high, Low, High Severity and most of all Enhanced Regrowth Low. About half of the burnt area pixels in Meru and Ontulili are mainly indicated by colours of the two vegetation regeneration classes: Enhanced Regrowth Low and High. It is shown thus, that forest stations do not tend to burn significantly during the fire-prone season in comparison to the low season.

As for the moorland, regrowth pixel frequency (proportional to its burnt area size) is slightly less than in the forest stations, suggesting temporal fragmentation of bigger fire events.

In terms of short temporal (fifteen years) fire regime it can be concluded that forest stations are driven by fires of similar intensity in both high and low seasons. The moorland shows a slightly more dynamic fire driven landscape in the fire prone season and less dynamism in the non-fire-prone season.

As can be seen in Figure 24 there is a clearer accumulation of Enhanced Regrowth High pixels with median NDVI value of 0.33 of the non-fire-prone season. Enhanced Regrowth Low (regeneration) is more pronounced for the fire-prone season, encompassing higher NDVI
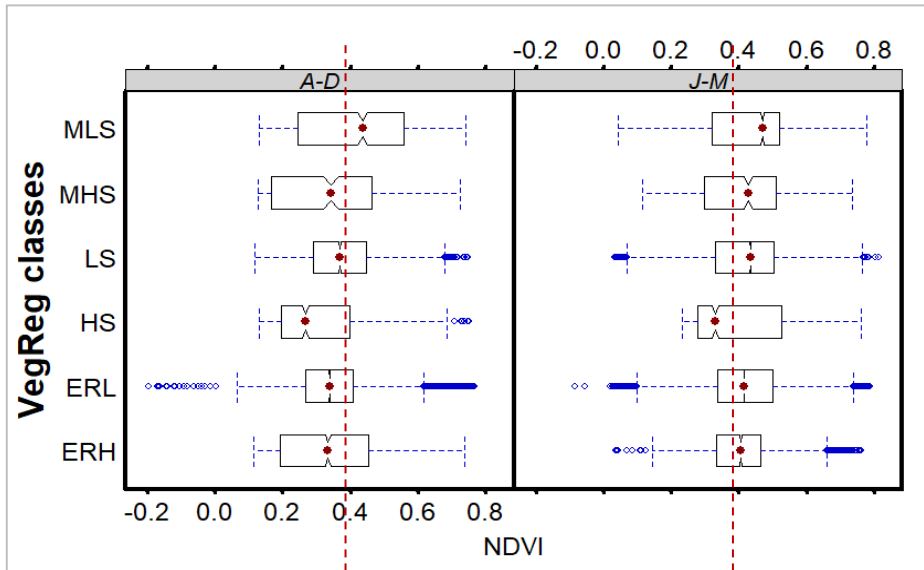
Fig. 24. VegReg classes pixel distribution over NDVI on burnt area as for fire seasons: April-December (left) and January-March (right). ERH- Enhanced Regrowth Low, ERL- Enhanced Regrowth High, HS- High Severity, LS- Low Severity, MLS- Moderate low Severity and MHS- Moderate high Severity. Median, 0.39 - red dashed line.

values (with median slightly over 0.4). A wider range of High Severity pixel spread can also be noted for the high season. In general, all VegReg classes relate to higher NDVI values in case of January-March, whereas relatively lower NDVI values are typical for the April-December season. Higher NDVI values suggest forest and moorland vegetation, while lower values are (0.2-0.3) are identified with cropland.

Seasonality driven difference with respect to fire activity based on the 'combined Vegetation Regeneration-Burn Severity on burnt area' analysis cannot be significantly distinguishable for the forest stations and North of Marania. A difference of significance can be pronounced by including the moorland into the analysis.

3.3.4. Accessibility (roads ~ trails buffer)

Since it is strongly assumed and suggested that fire ignition is human caused [7, 11, 16], the questions how humans can reach the spatial locations of IS (spatial points) arises. Simplest answer is: on roads and trails.

One glance at the provided road density shapefile made clear that trails above the timberline and roads in most of the forest stations are either missing or non-existing. Accurate and actual GIS applicable map of trails, roads or trekking routes of the Mount Kenya region proved difficult to acquire and by the time of writing the thesis none could be found.

Mending accuracy and drawing additional roads, trails and paths resulted in an increased road density map, that was applied for the purpose of the present thesis. Unfortunately, in the southern part of the moorland above Hombe and in the forest stations between Hombe and Chuka, trails could not be reproduced due to imagery cloudiness.

Fig. 24. shows, that IS have a strong relation with roads and trails, most of the IS are directly in contact with the snake-like buffered lines. An exceptional situation can be seen in the southern part above Hombe in case of two IS points, the assumption that there is a trail line leading up to join a trekking path, cannot be proven. Some IS can be observed within Ontulili (O), Gathiuru (G), Mucheene (Mu) and Meru (Me) adjacent to the buffered roads. These ignition sources are related to forest plantations, cultivations located within the forest. About half of all IS are present outside the forest, on the agricultural land use dominated area,

28

North of Marania (M), underlining its importance. The most AF1 points are clustered in the forest of Mucheene and in its vicinity on the moorland. Accessibility of that area is facilitated by roads nearby.

On the April-December map is the lack of trails in the south, south-eastern part of the moorland, where six IS and a number of AF1 and 2 are located, an appealing feature (Fig. 25.). As for the rest of high altitudinal fire ignition sources related to area accessibility, roads ~ trails network offers sufficient coverage.

Fire prone seasonal IS show the same characteristics that were described above for the low seasonal ones. IS centres can be identified on the area North of Marania, in the forests of Ontulili, Gathiuru and Marania. Forest stations with less IS are Mucheene, Meru, Ruthumbi, Chogoria, Chuka and Irangi. Because land use practices such as forest plantations mixed cultivation and cattle grazing are more concentrated during high fire season (Ngugi, written comment), 'seasonal weighted importance of accessibility' is accordingly more pronounced in the forest stations impacted by fires of the fire-prone season. A complete analysis regarding the moorland could not be performed due to technically uncompleted roads ~ trails network map.

The relation between roads ~ trails and Ignition Classes in preference to IS is simple. If fire events start with human induced ignitions as is the case in this thesis: the more roads ~ trails are crossing the region the easier to access larger areas (proportional to the region), consequently the more likely that more frequent human caused fire events occur on wider/larger areas of the region.
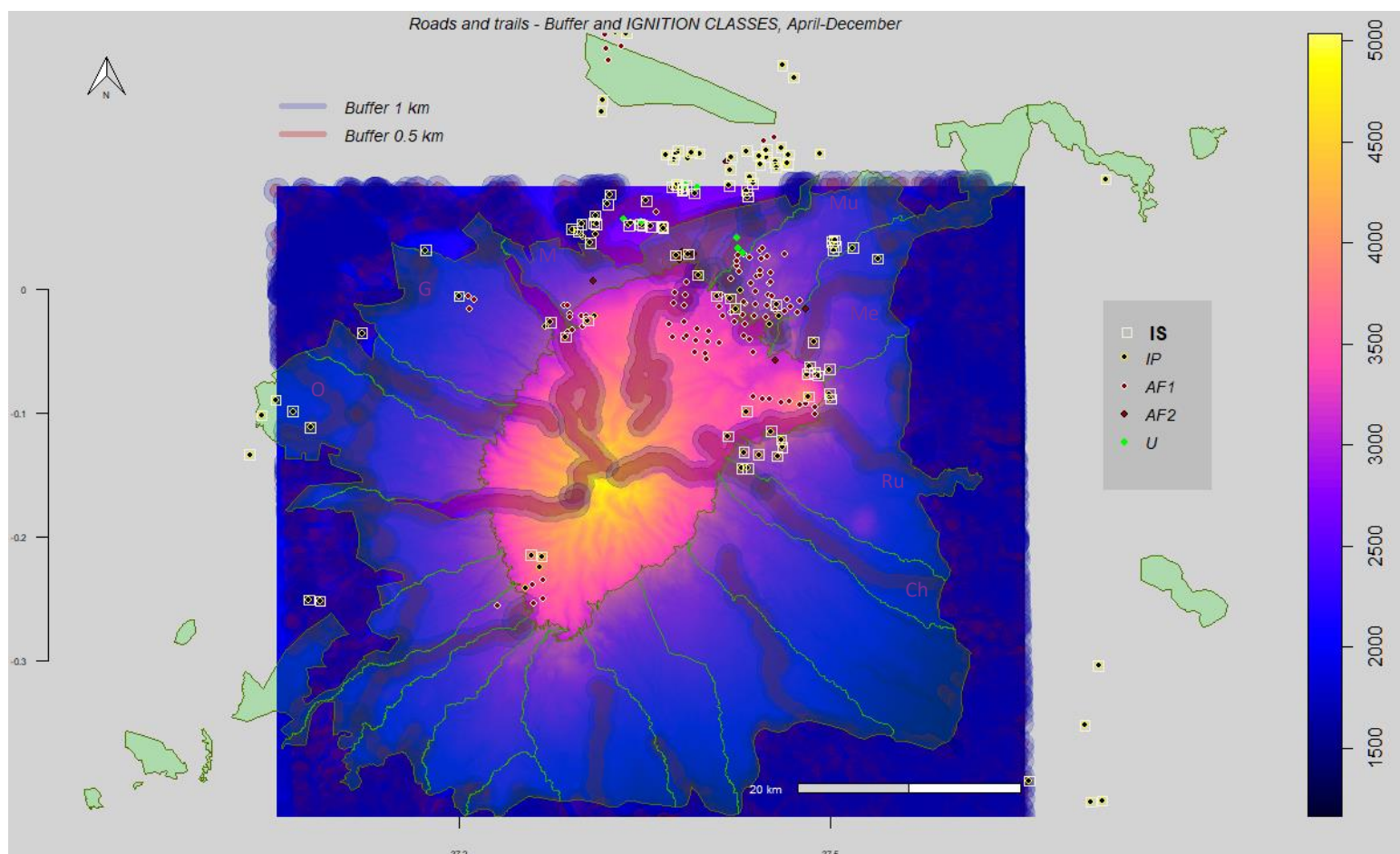
Fig. 25. Mount Kenya region's buffered roads ~ trails map, April-December. Ignition Sources represented by white rectangle. Ignition Classes: Ignition Point, After Fire 1, After Fire 2 and Unclear are denoted with symbols to be seen in the legend box. 500 m buffer expressed by red transparent line, displayed under 1000 m blue transparent buffer line. Forest stations: G represents Gathiuru, O Ontulili, M Marania, Mu indicates Mucheene, Me Meru, Ru Ruthumbu and Ch Chogoria.
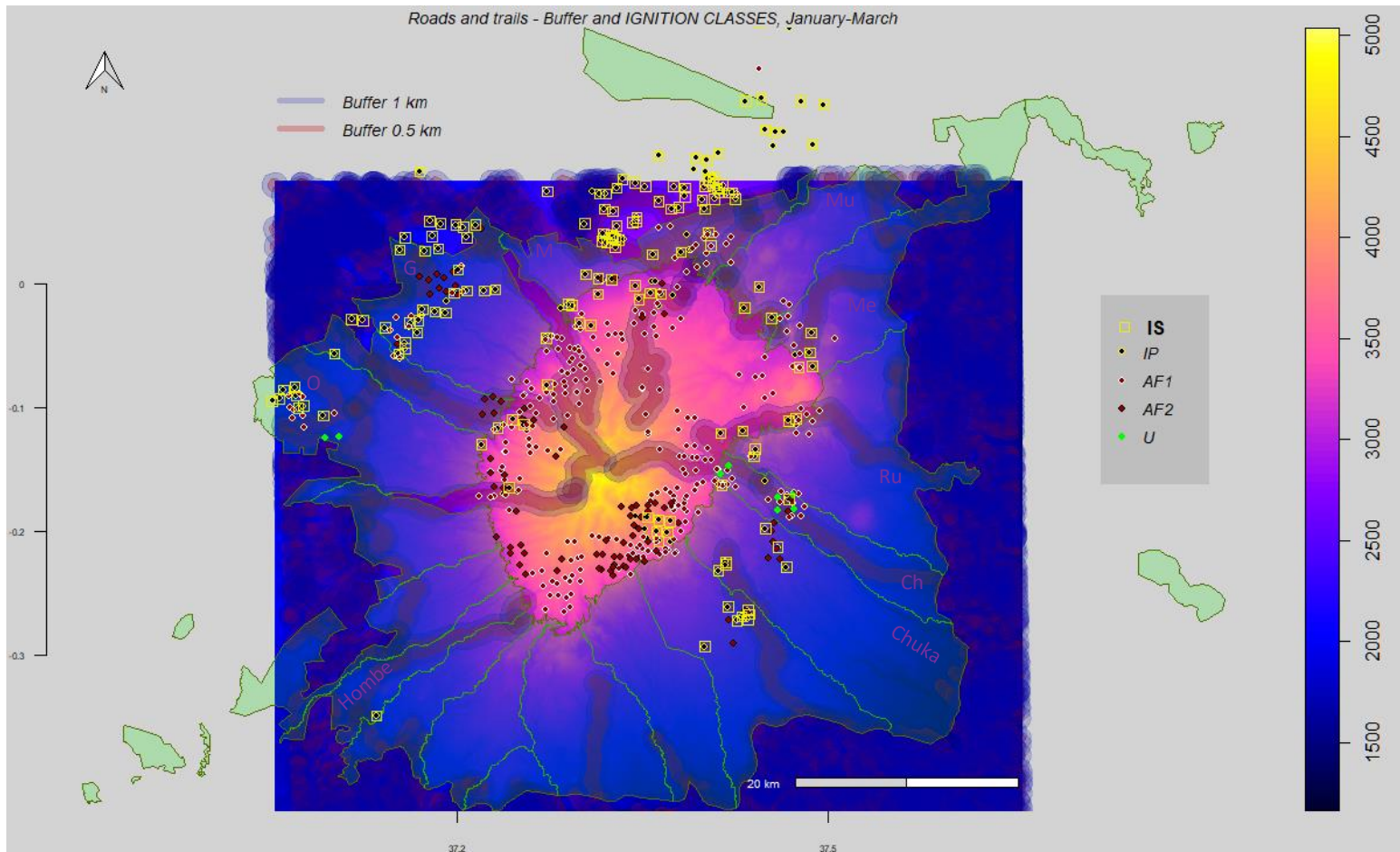
Fig. 26. Mount Kenya region's buffered roads ~ trails map, January-March. Ignition Sources represented by white rectangle. Ignition Classes: Ignition Point, After Fire 1, After Fire 2 and Unclear are denoted with symbols to be seen in the legend box. 500 m buffer expressed by red transparent line, displayed under 1000 m blue transparent buffer line. Forest stations: G represents Gathiuru, O Ontulili, M Marania, Mu indicates Mucheene, Me Meru, Ru Ruthumbu and Ch Chogoria.

3.4. > summary(results)

Bimodal fire seasonal theory was confirmed by **FO frequency** spatio-temporal distribution analysis (map), as well as by the results of combined **fire density and Mean to Variance Ratio** analysis. Furthermore, this dual seasonality was highlighted by the quantified **Burnt Area** monthly distribution analysis.

Spatial Point Pattern analyses (**G- and Ripley's K-functions**) have shown clustering FO pattern for very short distances (10-20 m) and for relatively short distances up to 300-400 m likewise.

Both, low and high seasonal IS spatial spreads and their **Kernel Density** concentration (after FO reclassification process) expressed an unexpected overlapping. IS tends to behave similarly over the study area irrespectively of in which season they occur.

High seasonal fire events consume in general (verified on 15-year-long scale) larger areas in the study region, especially on the moorland. In the forest stations, there is a clear season driven differentiation to be observed regarding **burnt area sizes**. The frequency and the number of fire events are, of course, higher in the January-March period. Still, as far as forested burnt area sizes concerned, seasons tend to be in balance with each other.

30

Land use changes were obtained from the stacked imagery of NDVI relevant band images and the NDVI image itself. **Pixel Ident Distribution** results show separate clustering of grass-, cropland and forest pixels for the year 2000 image, while the 2016 stacked image presents grass-, cropland and forest pixels overlapped in a similar shape and distribution. Moreover, the slight shift towards higher **NDVI** values indicate a trend of increasing assimilation, suggests a process of getting more healthier vegetation.

With regard to the combined **Vegetation Regeneration-Burn Severity** analysis: a seasonality driven difference in fire activity assessed on burnt area could not be detected.

The **roads ~ trails buffer** analysis suggests that the more roads ~ trails crossing the area, the more likely that more frequent human caused fire events occur on wider/larger areas of the study region.

4. Discussion and conclusions

Fire is one of the most important driving factors, threatening the Mount Kenyan ecosystem and it will surely remain so. Its effects will very likely be intensified in the future under the impacts of climate change.

Three questions were specified in the beginning of this thesis. The process of attempt to determine answers as accurate as possible was described up to present. In this section are the conclusive answers formulated.

(I) What are the spatial characteristics of the Mount Kenya fire regime and how can they be quantified?

- The ***dual seasonality (high and low fire seasons)***, confirming Poletti's work [16], marking spatial characteristics of fire regime, quantified by spatio-temporal fire frequency, density and burnt area analysis. The extent of the region's fire regime and its spatial variability covers not only the forest stations and the moorland, but the area North of Marania.

- The FO ***clustering pattern characteristics***, quantified by G and K-function methods of SPPA. The nearest neighbour distance test of the G-function showed strong clustering up to 12 m, irrespective to seasonality. It means either that MODIS detects FO very likely on the same spot or FO happens very likely on the same spot in different time. The MODIS detection hypothesis is more likely.

  The K-function revealed same clustering characteristics up to 350-400 m, suggesting the same conclusions as was described previously in case of the G-function.

(II) Which spatial patterns can be identified in relation to human activities (direct-ignition source and indirect-burnt area, fire severity, vegetation regeneration and NDVI) and how fire regime (I) is effected by them?

- Clustering patterned ***FO***, implying at spatial locations where human activities are frequent. Spatial random ***IS*** and ***AF1***, both are the result of the FO reclassification

process. **Fire event**(s) visualized by spatial combination of IS and AF1, marking the spatial fire spread of a given fire event. IS were related to *roads ~ trails* so as to verify spatial human accessibility. Human caused fires (IS) occur in the close neighbourhood of roads and trails. The resulting maps of the *roads ~ trails buffer analysis* clearly determine: the higher **roads ~ trails density** is, the easier to access (newly) opened up areas by (newly built) roads. On these areas with no regard to their location (forest, moorland), it is very likely that more frequent fire events will follow

- Clustering spatial distribution of *burnt area* directly related to IS, encompassing fire spreads of fire events. The more the ignitions are, the higher the probability for a fire event in both seasons. Human induced wild fire (any fire) can burn depending on seasonality and connected weather-fuel variables large areas. Clustering pattern of burnt area implies at fire-prone locations where human activities are practiced. Here, **roads ~ trails density** plays an essential role, as described above. It was shown that road density does not belong to the major factors limiting burnt area in Southern Africa [42]. However, it is not the case at Mount Kenya.

    High fire season is marked with more frequent moorland fire events burning larger areas (bigger fires), keeping up the characteristics of dual seasonality, unlike it is stated by Downing et al. [11]. High seasonal forest fire events are more frequent, burning approximately similar sized areas as less frequent forest fire events during the April-December period.

- ***Combined Vegetation Regeneration-Burn Severity, verified on burnt area*** results show no seasonality driven difference in fire activity. The spatially aggregated pattern of burnt areas are directly linked to roads ~ trails density, thus indirectly to human activities.

    By high seasonal fires burnt forest landscape tends to be as dynamic and active as low seasonal fire driven forest landscape. Whereas the moorland embodies a more dynamic, by large fire events determined landscape during the fire-prone season and transforms into a slightly less active fire by smaller fire events driven landscape during the low season.

    Increasing human caused fires impact the fire cycle (burning-regrowth). Depending on the cycle-interval, fire can either accelerate or hinder vegetation from regrowth. Mount Kenya's vegetation tends to be fire adaptive with quick response of growth on fire events, that is why classes of burn severity and vegetation regeneration are cumulatively present.

    Fire regime effects vegetation and in return vegetation affects fire regime. Further researches are needed to gain understanding how this interaction influences this fragile ecosystem and what effects it can have on essential ecosystem services like providing fresh water.

- No spatial patterns could be identified by the NDVI and PID analyses, because neither the change of NDVI values nor the clustering, non-clustering characteristics of PID could be spatially related to activities practiced by humans, which cause fire.

(III) How is the quality and quantity of available remote sensing (RS) data to provide necessary information relating questions (I) and (II) above?

- It is difficult to reflect on the qualitative part of the question due to lack of comparable studies in field of afro-alpine environment.

  As described in section 2.2.2. overall fire detection performance of Collection 5 Terra MODIS is acceptably accurate, but in Central-Africa (including Mount Kenya region) proofed to be very accurate. Fire occurrence based analyses were performed with this data.

  Accuracy of Collection 5 MCD54A1 Burned Area Product was praised over Collection 6 MCD64A1 as a better performer in detecting small fires in steep mountainous area [23]. The former product was used for burnt area assessment.

  The scientific legacy of Landsat 7 and ETM+ and Landsat 8 is enormous and far too numerous to mention for the extent of this thesis. Landsat satellite data were used for the calculations of NDVI images and ∆NBR (from which combined vegetation regeneration and burn severity analysis were derived). Field of selection was restricted partly by the SLC-off scanner issue of Landsat 7 ETM+, and partly by cloudiness in the imagery. The two Landsat images were selected with care and consideration, making the author to choose images from different years of the study period: 2000 and 2016. Still, the 2016 image shows some cloudy patches over the mountain. It can have an error-raising effect on the NDVI and PID analyses, which turned out to be non-responsive (irrelevant) to questions (I) and (II).

  Apart from the qualitatively influenced quantitative restriction just mentioned, the quantitative availability of RS data for the scope of this thesis is thoroughly satisfactory.

5. Recommendations

1. In general

Fire danger sign posting at frequent distances along trails and roads, especially nearby fire-prone areas, and awareness raising by all possible means (workshops, organized education programs, distribution of simple maps) are suggested. Supervising / monitoring (a system to be created, which is sensitive to changes and flexible towards pending optimization processes) land preparatory activities on cultivated lands and in plantations within forest stations are highly recommended. Maintaining roads and trails (combined with intensified monitoring activities in the fire prone months) so as to lead people on monitored trails is considered as essential. Without clear pre-signing roads and trails, maintenance efforts will lose from their efficiency, so it is also essential. Fire management is strongly recommended

for the **whole year**, holding seasonal characteristics (considering January-March as highly fire-prone and July-September as highly fire-sensitive months) before the eye.

Further recommendations include the creation and implementation of a fire danger map based on various up to dated meteorological data (recently found availability: http://wlrc-ken.org/data/timeseries/home) and classified fuel types. An understanding of the underlying processes of fire regime as described on the pages of this thesis, might support this attempt.

Last but not least, it is very important that the author of the present thesis does *NOT recommend* building new roads or trails.

5.2. In particular

For the future, fire management recommendations described in previous section are advised to be based on an extended map version of forest station boundaries, called Mount Kenya Future Forest Stations (Fig. 26.), covering the Mount Kenya Reserve. The numbers of FO and IS are indicated with italic letters, IS are underlined. The expanded boundaries were drawn considering the original spatial distribution of the forest stations and a possible fair distribution of the moorland (relative to sizes of the distinct forest stations). The assessment of fire prone areas by implementing the ameliorated GIS data provided here in combination
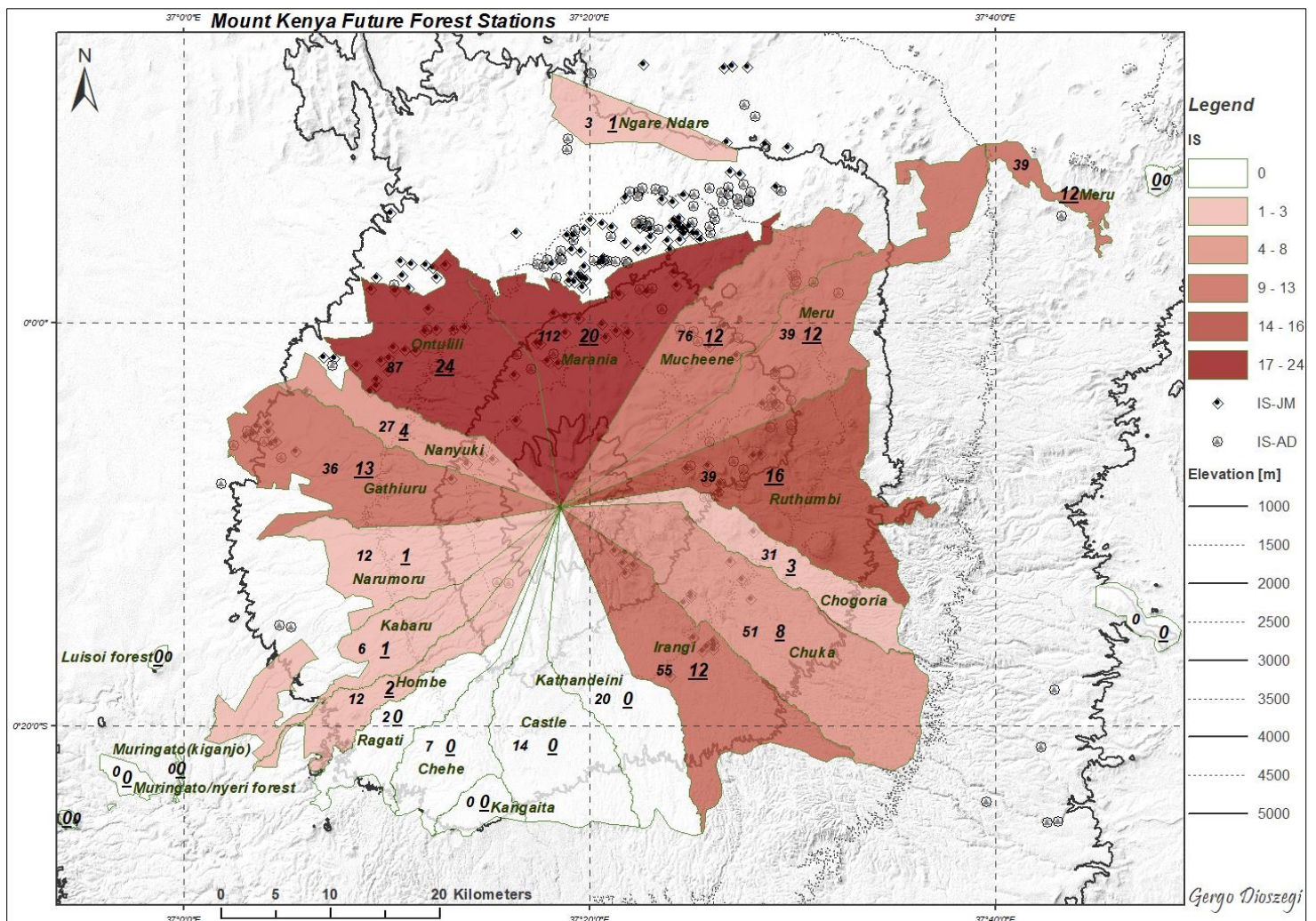
Fig. 27. For fire management and research recommended Future Forest Station (FFS). Ignition Sources frequency indicated by shading red for each forest stations. High seasonal IS displayed by in-quadrat-black dots, low seasonal IS by in-circle-grey triangles. Sum of MODIS FO (italic) and IS (italic, underlined) are shown for each FFF. Period 2001-2015. Map is available and ready to be implemented.

of available remote sensing data could be the next step for specific spatial modelling in the Mount Kenya region. Moreover, this new GIS applicable shapefile could be the base for the fire danger map.

At this stage the author of this thesis cannot tell whether the Future Forest Stations will be supportively useful, but dearly hopes that they will be used, re-used and will bring some help in raising awareness of fire's destructiveness and responsibility of keeping Mount Kenya's natural resources sustainably safe for future generations.

References

[1] Scott, A. (2000) The pre-quaternary history of fire. *Palaeogeography, Palaeoclimatology, Palaeoecology*. 164, 281-329

[2] Archibald, S.; Staver, A. C.; Levin, S. (2012) Evolution of human-driven fire regimes in Africa. *PNAS*. January 2012, 109 (3), 847-852

[3] McKenzie, D.; Miller, C.; Falk, D. (2011) The Landscape Ecology of Fire. Springer, New York

[4] Archibald, S.; Scholes, R.; Roy, D.; Roberts, G.; Boschetti, L. (2010) Southern African fire regimes as revealed by remote sensing. *Int. Journal of Wildland Fire.* 19, 861-878

[5] Ellison, D.; Morris, E. C.; Locatelli, B.; Shei, D.; Cohen, J.; Murdiyars, D.; Gutierrez, V.; van Noordwijk, M.; Creed, F. I.; Pokorny, J.; Gaveau, D.; Spracklen V.; Bargués, D.; Tobella, A.; Ilstedt, U.; Teuling, J. A.; Gebreyohannis Gebrehiwot, S.; Sands, C. D.; Muys, B.; Verbist, B.; Springgay, E.; Sugandi, Y.; Sullivan, A.C. (2017) Trees, forests and water: Cool insights for a hot world. *Global Environmental Change*. March 2017, 43, 51-61

[6] Viviroli, D.; Dürr, H.; Messerli, B.; Meybeck, M.; Weingartner, R. (2007) Mountains of the world, water towers for humanity: Typology, mapping, and global significance. *Water resources research.* 2007, 43 (7), 1-13

[7] Nyongesa, K. (2015) Fire Management in Forests and National Parks of Kenya. Master thesis, University of Natural Resources and Life Sciences, Vienna

[8] Jacob, M.; Annys, S.; Frankl, A.; de Ridder, M.; Beeckman, H.; Guyassa, E.; Nyssen J. (2015) Tree line dynamics in the tropical African highlands – identifying drivers and dynamics. *J Veg Sci*, 2015, 26 (1), 9-20

[9] Rucina, S.M.; Muiruri, V.M.; Kinyanjui, R.N.; McGuiness, K.; Marchant, R. (2009) Late Quaternary vegetation and fire dynamics on Mount Kenya. *Palaeoecology.* 283, 1-14

[10] Bussmann, R.W. (2006) Vegetation zonation and nomenclature of African Mountains- An overview. *Lyonia*, 11, 41-66

[11] Downing, T.A.; Imo, M.; Kimanzi, J. (2017) Fire occurrence on Mount Kenya and patterns of burning. *GeoResJ*, June 2017, 17-26

[12] Aldersley, A.; Murray, S.J.; Cornell, S.E. (2011) Global and regional analysis of climate and human drivers of wildfire. *Sci Total Environ*. 409 (18), 3472-3481

[13] Sanderson, E.W.; Jaiteh, M.; Levy, M.A.; Redford, K.H.; Wannebo, A. V.; Woolmer; G. (2002) The human footprint and the last of the wild: The human footprint is a global influence on the land surface, which suggests that human beings are stewards of nature, whether we like it or not. *Bioscience.* 52, 891-904

[14] Wesche, K.; Miehe, G.; Kaeppeli, M. (2000) Significance of Fire for Afroalpine Ericaceous Vegetation. *Mountain Research and Development.* Nov 2000, 20 (4), 340-347

[15] Imo, M. (2012) Forest Degradation in Kenya: Impacts of Social, Economic and Political Transitions. *Kenya: Social, Environmental and Political Issues.*, Editors: Adoyo, J.W. and Wangai, C.I., Nova Publishers, 1-38

[16] Polletti, C. (2016) Characterization of forest fires in the Mount Kenya region (1980-2015). Master thesis, University of Padova

[17] Henne Stephan, Junkermann Wolfgang, Kariuki Josiah, Aseyo John, Klausen Jörg, 2008. Mount Kenya Global Atmosphere Watch Station (MKN): Installation and Meteorological Characterization. *Juornal of Applied Metereology and Climatology.* 47, 2946 – 2962

[18] UNESCO (2013) Decisions Adopted by the World Heritage Committee at its 37th session (Phnom Penh, 2013). Phnom Penh, Cambodia, 156-159

[19] Nyongesa, K. (2016) Description of Mount Kenya Vegetation, manuscript

[20] Loboda, T. V. and Csiszar, I.A. (2007) Reconstruction of Fire Spread within Wildland Fire Events in Northern Eurasia from the MODIS Active Fire Product. *Global and Planetary Change.* 56, 258-273

[21] Cheng, D.; Rogan, J.; Schneider, L.; Cochrane, M. (2013) Evaluating MODIS active fire products in subtropical Yucatan forest. *Remote Sensing Letters.* 4, 455-464

[22] de Klerk, H. (2008) A pragmatic assessment of the usefulness of the MODIS (Terra and Aqua) 1-km active fire (MOD14A2 and MYD14A2) products for mapping fires in the fynbos biome. *International Journal of Wildland Fire.* 17, 166-178

[23] Hantson, S.; Padilla, M.; Corti, D.; & Chuvieco, E. (2013). Strengths and weaknesses of MODIS hotspots to characterize global fire occurrence. Remote Sensing of Environment. 131, 152–159

[24] Giglo, L.; Schroeder, W.; Justice, C.O. (2016) The collection 6 MODIS active fire detection algorithm and fire product. *Remote Sensing of Environment.* 1 June 2016, 178, 31-41

[25] Tsela, P.; Wessels, K.; Botai, J.; Archibald, S.; Swanepoel, D.; Steenkamp, K.; Frost, P. (2014) Validation of the Two Standard MODIS Satellite Burned-Area Products and an Empirically-Derived Merged Product in South Africa. *Remote Sensing.* 6, 1275-1293

[26] Fornacca, D.; Ren, G.; Xiao, W. (2017) Performance of Three MODIS Fire Products (MCD45A1, MCD64A1, MCD14ML), and ESA Fire_CCI in a Mountainous Area of Northwest Yunnan, China, Characterized by Frequent Small Fires. *Remote Sensing.* 9*,* 1131 - article number

[27] van Wagtendonk; J.W.; Root, R.R.; Key, C.H. (2004) Comparison of AVIRIS and Landsat ETM+ detection capabilities for burn severity. *Remote Sensing of Environment.* 92, 397-408

[28] Bivand, R.S.; Pebesma, E.J.; Gomez-Rubio, V. (2008) Applied spatial data analysis with R. http://gis.humboldt.edu/OLM/r/Spatial%20Analysis%20With%20R.pdf

[29] Baddeley, A. and Gill, R. D. (1997) Kaplan-Meier estimators of distance distributions for spatial point processes. *Annals of Statistics.* 25, 263-292

[30] Ripley, B.D. (1977) Modelling spatial patterns (with discussion). *Journal of the Royal Statistical Society.* Series B, 39, 172-212

[31] Ripley, B.D. (1988) Statistical inference for spatial processes. Cambridge University Press, 1988

[32] Baddeley, A. (2010) Analysing spatial point patterns in R. Workshop Notes. Version 4.1, December 2010

[33] Key, C.H. and Benson, N.C. (2006) Landscape Assessment (LA). *FIREMON: Fire Effects Monitoring and Inventory System*. Fort Collins, CO: US department of Agriculture, Forest service, Rocky Mountain Research Station, Gen.Tech Rep. RMRS-GTR-164-CD

[34] Olea, R.A. and Pawlowsky-Glahn, V. (2009) Kolmogorov-Smirnov test for spatially correlated data. *Stochastic Environmental Research and Risk Assessment.* 23(6), 749-757

[35] Finney, M.A. (2004) FARSITE: Fire Area Simulator - Model Development and Evaluation. USDA Forest Service Research Papers RMRS-RP-4, Missoula, MT, 2004

[36] Sullivan, A.L. (2009) Wildland surface fire spread modelling, 1990–2007. 1: Physical and quasi-physical models. *International Journal of Wildland Fire.* 18, 349–368

[37] Moran, P. A. P. (1950) Notes on Continuous Stochastic Phenomen. *Biometrika*. 37(1), 17-23

[38] Rogers, J.L. and Nicewander W. A. (1988) Thirteen Ways to Look at the Correlation Coefficient. *The American Statistician*. 42(1), 59-66

[39] Harris, R. (2013) An Introduction to Mapping and Spatial Modelling in R. 10.13140/RG.2.1.1691.1847. University of Bristol

[40] Keeley, J.E. (2009) Fire intensity, fire severity and burn severity: a brief review and suggested usage. *International Journal of Wildland Fire* 18(1), 116-126

[41] Archibald, S., Roy, D.P., Van Wilgen, B.W., Scholes, R. J. (2009) What limits fire? An examination of drivers of burnt area in Southern Africa. *Global Change Biology* 15, 613–630